

## APPENDIX D

KARAMCHANDANI, P., ZHANG, Y., AND C. SEIGNEUR, 1999. SIMULATION OF SULFATE FORMATION IN THE MOHAVE POWER PLANT PLUME. REPORT PREPARED FOR THE ELECTRIC POWER RESEARCH INSTITUTE, JANUARY

# **SIMULATION OF SULFATE FORMATION IN THE MOHAVE POWER PLANT PLUME**

Final Report, January 1999

Prepared by

Atmospheric & Environmental Research, Inc.

2682 Bishop Drive, Suite 120

San Ramon, CA 94583

Prakash Karamchandani

Yang Zhang

Christian Seigneur

Prepared for

**Electric Power Research Institute**

3412 Hillview Avenue

Palo Alto, California 94304

EPRI Project Managers

M.A. Allan

P. Saxena

Environment Division

## Table of Contents

1.	Introduction .....	1-1
2.	Technical Approach .....	2-1
2.1	Summary of Approach .....	2-1
2.2	Chemistry of Power Plant Plumes.....	2-2
2.3	The Reactive and Optics Model of Emissions (ROME).....	2-3
2.4	Previous Applications and Evaluation of ROME.....	2-5
2.5	Preparation of Model Inputs.....	2-7
2.5.1	Meteorology and dispersion .....	2-8
2.5.2	Background concentrations .....	2-11
3.	Base Case Simulations .....	3-1
3.1	Selection of Trajectories.....	3-1
3.2	Description of Trajectories .....	3-4
3.3.	Results .....	3-6
4.	Additional Studies .....	4-1
4.1	Effect of MPP NO <sub>x</sub> Emissions .....	4-1
4.2	Effect of Overlapping Puffs .....	4-3
4.3	Effect of 90% Reduction in MPP SO <sub>2</sub> Emissions .....	4-7
4.4	Effect of Las Vegas Urban Plume.....	4-7
4.5	Effect of Cloud Updraft Velocity .....	4-8
4.6	Effect of Background Concentrations .....	4-9
4.7	Estimation of Maximum Sulfate Concentrations in the Grand Canyon Region .....	4-15
4.8	Effect of Clouds .....	4-20
4.9	Estimation of Maximum Hourly MPP Sulfate Contribution .....	4-21

**Table of Contents (continued)**

5. Summary and Conclusions ..... 5-1

6. References ..... 6-1

## List of Tables

Table 2-1.	Emissions from the Mohave Power Plant .....	2-9
Table 2-2.	Range of concentrations measured during August 6 to 16, 1992 in the Project Mohave area .....	2-12
Table 2-3a.	PAN concentrations measured at a number of locations.....	2-14
Table 2-3b.	Formaldehyde and acetaldehyde concentrations measured at a number of locations .....	2-15
Table 3-1.	Background concentrations (in ppb unless otherwise indicated) for the base case simulations .....	3-3
Table 3-2.	Description of selected trajectories traveling from the Mohave Power Plant to Meadview.....	3-5
Table 3-3.	Description of selected trajectories traveling from the Mohave Power Plant to Hopi Point.....	3-7
Table 3-4.	Base case results for Meadview .....	3-8
Table 3-5.	Base case results for Hopi Point.....	3-10
Table 4-1.	High background concentrations (in ppb unless otherwise indicated)...	4-10
Table 4-2.	High background results for Meadview .....	4-11
Table 4-3.	High background results for Hopi Point .....	4-16
Table 4-4.	Approximate maximum MPP sulfate concentrations in Grand Canyon region relative to calculated receptor concentrations.....	4-18

## List of Figures

Figure 4-1.	The ratio of the plume SO <sub>2</sub> gas-phase oxidation rate to the ambient rate as a function of plume SO <sub>2</sub> concentration .....	4-2
Figure 4-2.	The ratio of the instantaneous sulfate concentration in the plume when MPP NO <sub>x</sub> = 0 to the base case value as a function of travel time .....	4-4
Figure 4-3.	The ratio of the instantaneous sulfate concentration in the plume for different MPP NO <sub>x</sub> values to the base case value as a function of travel time .....	4-6
Figure 4-4.	The ratio of the instantaneous plume sulfate concentration in the high background case to the corresponding values in the base case, as a function of travel time .....	4-13
Figure 4-5.	The ratio of the instantaneous plume H <sub>2</sub> O <sub>2</sub> concentration in the high background case to the corresponding value in the base case, as a function of travel time .....	4-14
Figure 4-6.	Instantaneous sulfate concentrations in the plume in the Grand Canyon region, relative to the instantaneous concentration at Hopi Point for puff 1479 .....	4-19

## 1. INTRODUCTION

Project MOHAVE is a regional haze attribution study to determine impacts of the Mohave Power Plant (MPP), a large coal-fired facility in southern Nevada, and other large sources on visibility at Grand Canyon National Park and other national parks and wilderness areas in the southwestern United States with federal visibility protection (Pitchford et al., 1997). The study is sponsored by the Environmental Protection Agency, Southern California Edison Company, and the National Park Service. EPRI is managing components of the scientific work for the Project MOHAVE sponsors. In addition, a large number of governmental, academic, and industrial organizations have been involved in various aspects of the study such as monitoring (including two intensive monitoring periods from 1/15/92 to 2/14/92 in winter and from 7/12/92 to 8/31/92 in summer), modeling, and data analysis.

Several modeling approaches have been and are being used to perform the source attribution analysis. These include receptor models (e.g., Ames and Malm, 1997; Eatough et al., 1997a) and source-oriented transport/dispersion/chemistry models such as HAZEPUFF (Latimer, 1993), VISHWA (Karamchandani et al., 1996; Venkatram et al., 1997), and CALPUFF (Vimont, 1997). In this report, we describe a modeling approach that combines detailed representations of plume dynamics and plume chemistry to determine the conversion of MPP SO<sub>2</sub> emissions to sulfate and the contribution of MPP sulfate to measured sulfate concentrations at a number of locations in the Grand Canyon region. Plume dynamics was simulated by Lu and Yamada (1998) using a primitive equation meteorological model (Yamada and Bunker, 1988) and a state-of-the-science puff dispersion model. These simulations are described by Yamada (1997) in a companion report. Plume chemistry, which is discussed in this report, was simulated with a reactive plume model, referred to as the Reactive and Optics Model of Emissions (ROME) (Seigneur et al., 1997a).

ROME includes state-of-the-science formulations of the governing atmospheric transformation processes, including gas- and aqueous-phase reactions, gas-liquid equilibria, gas/particle equilibria, and aerosol dynamics and chemical composition (Seigneur et al., 1997a). The model uses a Lagrangian approach to simulate the transport

and dispersion of the MPP plume, and simulates the gas- and aqueous-phase chemical reactions that occur as the plume mixes with the background air (We define background air as the air outside the plume). Chemical concentrations in the background air were obtained from surface and aircraft measurements during the summer intensive period of Project MOHAVE as well as from a literature review for chemicals that were not measured during the field study.

Information on plume dynamics (width and vertical mixing as a function of downwind distances) and background meteorology (location, temperature, pressure, relative humidity, cloud liquid water content) was derived along the trajectory from the results of Lu and Yamada (1998). As described in the companion report, Lu and Yamada (1998) applied the three-dimensional atmospheric modeling system, HOTMAC/RAPTAD (Higher Order Turbulence Model for Atmospheric Circulation/Random Puff Transport and Diffusion) to simulate the wind, turbulence and tracer gas concentrations during the summer intensive period of Project MOHAVE.

We present in this report the plume chemistry simulations that were conducted for selected days of a 11-day period in August 1992, when transport of the MPP plume towards the Grand Canyon was noted from tracer measurements. We describe in Section 2 our overall approach for conducting the plume chemistry simulations. The base case simulations are presented in Section 3. Section 4 presents additional studies that were performed to examine the effect of background concentrations on the results, as well as to examine plausible hypothetical scenarios that would increase the amount of MPP contribution to sulfate concentrations.

## 2. TECHNICAL APPROACH

### 2.1 Summary of Approach

As discussed in more detail in Section 2.2, SO<sub>2</sub> oxidation rates in a power plant plume can be significantly different from ambient background oxidation rates, because NO<sub>x</sub> concentrations that affect oxidant levels in the plume are significantly different in the plume and in the background. Plume SO<sub>2</sub> oxidation rates are strong functions of the background chemical concentrations, plume dispersion, and interactions of the plume with fog and clouds. Furthermore, plume oxidation rates will vary with time because (1) the gas-phase reaction is a function of OH concentrations that are affected by photochemical activity, (2) the aqueous-phase reaction with H<sub>2</sub>O<sub>2</sub> is typically oxidant-limited in a plume and will proceed rapidly but will stop when H<sub>2</sub>O<sub>2</sub> is exhausted, and (3) the aqueous-phase reactions with O<sub>2</sub> (catalyzed by Fe and Mn) and O<sub>3</sub> are self-limiting because their rates decrease with decreasing pH. In addition, the aqueous-phase conversion processes typically lead to non-linear relationships between SO<sub>2</sub> and sulfate. Such non-linear relationships cannot be simulated with constant conversion rates. Thus, it is necessary to simulate these chemical processes explicitly to properly represent the conversion of SO<sub>2</sub> to sulfate in the MPP plume.

The approach that we adopted here was to use a reactive plume model with a detailed treatment of the gas-phase, particulate-phase, and droplet-phase chemical reactions that govern the oxidation of SO<sub>2</sub> to sulfate. A description of the model and previous performance evaluations of the model are provided in Sections 2.3 and 2.4, respectively.

The model was applied for the period of August 6 to August 16, 1992. This period was selected by the Project MOHAVE Technical Committee because it corresponded to a period of intensive measurements during summer (summer meteorology was considered to be more conducive to Mohave power plant impacts in the Grand Canyon area than winter meteorology). The model requires meteorological and dispersion data, as well as background chemical concentrations, along the plume trajectory to perform the transport, dispersion and chemistry calculations. In addition,

emissions of SO<sub>2</sub>, NO<sub>x</sub>, tracer, and trace metals such as iron and manganese are also required to specify the initial concentrations in the plume near the stack. Section 2.5 provides a description of how some of the above data requirements were met. Wherever information needed to conduct the simulations was not available at all (either from the databases available to us or from a review of the literature) or was available in the form of a range, we deliberately chose conditions that would provide an estimate of the largest reasonable MPP contribution to the sulfate concentration at the receptor. Section 2.5 provides additional details.

## 2.2 Chemistry of Power Plant Plumes

The oxidation of SO<sub>2</sub> to sulfate in a power plant plume cannot be simulated by assuming a constant oxidation rate expressed in percent SO<sub>2</sub> conversion per hour. The gas-phase oxidation will initially proceed more slowly in a power plant plume than in the background air because the presence of high concentrations of NO and NO<sub>2</sub> in the plume leads to lower O<sub>3</sub> and OH radical concentrations in the plume than in the background (OH radicals and O<sub>3</sub> are the oxidants that drive acid formation primarily during daytime and nighttime, respectively). As the plume mixes with the background air and gets diluted, the rate of SO<sub>2</sub> oxidation in the plume approaches that in the background. In the case where the background photochemistry is NO<sub>x</sub> limited, the plume SO<sub>2</sub> oxidation rate may temporarily exceed the background oxidation rate. In contrast, gas-phase SO<sub>2</sub> oxidation rates in smelter plumes are similar to background oxidation rates (e.g., Richards et al., 1982; Hudischewskyj and Seigneur, 1989) because NO<sub>x</sub> emissions from smelters are minimal.

The aqueous-phase oxidation will also proceed initially more slowly in the plume than in the background, because the primary aqueous-phase oxidant, H<sub>2</sub>O<sub>2</sub>, reacts first with background SO<sub>2</sub>; furthermore, plume nitric acid and nitrate formation leads to lower pH in the plume than in the background, resulting in lower aqueous-phase SO<sub>2</sub> oxidation rates by O<sub>3</sub> and O<sub>2</sub> (catalyzed by Fe and Mn).

SO<sub>2</sub> oxidation rates derived from aircraft studies of the Navajo Generating Station (NGS) plume (Richards et al., 1981) and the MPP plume (Hegg et al., 1985) confirm that

plume SO<sub>2</sub> oxidation rates are low particularly for plume ages of a few hours. For example, for the early morning of July 13, 1979, Richards et al. (1981) derived average plume SO<sub>2</sub> oxidation rates of 0.03% per hour at about 59 km downwind of NGS. Between 59 and 89 km downwind, when the plume became diluted, they derived oxidation rates of 0.8% per hour, resulting in an average SO<sub>2</sub> oxidation rate of 0.36% per hour between the stack and 89 km. Similarly, Hegg et al. (1985) conducted multiple airborne studies of the Mohave plume during the winters and summers in the late 1970's through 1980. Because of the presence of NO<sub>x</sub> in the plume, the conversion of SO<sub>2</sub> to sulfate was slow, averaging 0.6% per hour. This is an aggregate average covering winter and summer, including monsoonal cloudy type days during the summer.

Hudischewskyj and Seigneur (1989) used a reactive plume model to perform NGS and MPP plume simulations for the same periods as the aircraft measurements by Richards et al. (1981) and Hegg et al. (1985), respectively. They concluded that the background air of the region did not provide sufficient oxidant concentrations to lead to high conversion rates of NGS or MPP SO<sub>2</sub> to sulfate. Conversely, simulations of a power plant plume located in an urban environment resulted in much larger conversion of SO<sub>2</sub> to sulfate than in the NGS or MPP plumes (Hudischewskyj and Seigneur, 1989).

Richards et al. (1982) conducted airborne measurements in the plumes of the San Manuel and Douglas smelters in Arizona during September 1981. They found SO<sub>2</sub> conversion rates in these plumes to be comparable to background rates and about a factor of ten larger than those in coal-fired power plant plumes in the southwestern U.S. The lower rates in power plant plumes as compared to smelter plumes were attributed to the higher NO<sub>x</sub> emissions in the power plant plumes. These findings were confirmed in simulations performed for the San Manuel smelter by Hudischewskyj and Seigneur (1989).

### **2.3 The Reactive and Optics Model of Emissions (ROME)**

The Reactive and Optics Model of Emissions (ROME) is a reactive plume model that includes state-of-the-science formulations of atmospheric chemistry, aerosol dynamics, and plume rise and dispersion using second-order closure algorithms (Seigneur

et al., 1997). The model uses a Lagrangian approach to simulate the dispersion of a plume emitted from a stack and advected by the mean wind flow, and simulates the chemical reactions that occur as the plume mixes with the background air. The model consists of a two-dimensional array of contiguous cells that is perpendicular to the wind direction. The cells can expand horizontally according to a normal distribution for inert species. The vertical depths of the cells remain constant during a given simulation.

Reactive chemical species undergo chemical reactions within each cell and diffuse between contiguous cells and between the cells and the background according to a Fickian diffusion algorithm. Concentrations of emitted inert species are assumed to follow a normal distribution. In addition, vertical diffusion and convection occur for all species (inert and reactive) since the vertical grid structure of the model does not change during a given simulation. A variety of options are available to specify or calculate the horizontal and vertical diffusion coefficients. For example, the model includes a state-of-the-science formulation for plume rise and dispersion using second-order closure algorithms. However, the plume dynamics modules of ROME were not used to specify plume dispersion because, as described in Section 2.5, we specified the physical characteristics of the plume using the results of Lu and Yamada (1998).

ROME also includes modules for gas- and aqueous-phase chemistries and gas-liquid equilibria, aerosol dynamics and chemical composition, dry and wet deposition, and atmospheric optics. The gas-phase chemistry of VOC,  $\text{NO}_x$  and photochemical oxidants is based on the most recent version of the Carbon Bond Mechanism IV (CBM 4.1; Gery et al., 1989 with subsequent revisions). The gas-phase oxidation of  $\text{SO}_2$  to sulfate is simulated using the kinetic expression of Atkinson and Lloyd (1984).

In the presence of clouds, the aqueous-phase chemistry module in ROME is activated. Cloud liquid water content can be prescribed either as an input or calculated internally in the model using a cloud microphysics module. The aqueous-phase chemistry module includes 30 irreversible reactions, 13 ionic equilibria, and 18 gas-liquid equilibria (Seigneur and Saxena, 1988). The three major pathways leading to  $\text{SO}_2$  oxidation in the aqueous-phase are included in the mechanism. These include oxidation by  $\text{H}_2\text{O}_2$ ,  $\text{O}_3$ , and  $\text{O}_2$  (catalyzed by trace metals such as iron and manganese). The oxidation of  $\text{SO}_2$  by  $\text{H}_2\text{O}_2$  has been shown to be very rapid (Hoffman and Calvert, 1985)

and SO<sub>2</sub> and H<sub>2</sub>O<sub>2</sub> typically do not coexist in atmospheric clouds (unless SO<sub>2</sub> is complexed as hydroxymethanesulfonic acid by formaldehyde). The aqueous-phase chemical mechanism in ROME simulates this titration of SO<sub>2</sub> with H<sub>2</sub>O<sub>2</sub>. The oxidation reactions of SO<sub>2</sub> with O<sub>3</sub> and O<sub>2</sub> are slower and have chemical kinetics that depend on the pH of the cloud droplets (Hoffman and Calvert, 1985; Martin, 1994). The ROME chemical mechanism uses the most recently available laboratory data to simulate these reactions.

The treatment of aerosol dynamics, particulate chemical composition, and plume optics was not used in the ROME simulations described here and, therefore, is not discussed further.

## **2.4 Previous Applications and Evaluation of ROME**

Since we used the results of Lu and Yamada (1998) to define the physical characteristics of the plume, such as plume width and vertical dispersion coefficients, and not the dispersion algorithms of ROME, we will focus most of our discussion on the evaluation of the chemistry component of ROME. However, since plume chemical concentrations depend on the plume physics, it is useful to review the performance of the plume dispersion algorithms which underlie the results of Lu and Yamada with respect to observed plume characteristics such as plume width. Gabruk et al. (1999) conducted an operational evaluation of the ability of ROME to simulate several plume physical and chemical variables, using an experimental data base that consisted of a total of 39 case studies from four field programs (VISTTA79, VISTTA81, NYSEG, and SEAPC). They used three different dispersion algorithms available in ROME: 1) the Pasquill-Gifford-Turner (PGT) empirical algorithm, 2) a first-order closure (FOC) time-averaged algorithm, and 3) a second-order closure (SOC) algorithm for instantaneous plume dispersion.

Gabruk et al. (1999) found that the SOC dispersion algorithm demonstrated better performance than both the PGT and FOC algorithms in the simulation of horizontal plume spread. Although the correlations to the observed widths were similar for all three

algorithms, the SOC algorithm had significantly less bias, a larger range of correlation, and more simulated plume widths within a factor of 2 of the observed values.

Of the four field programs studied by Gabruk et al. (1999), only the New York State Electric and Gas Corporation (NYSEG) 1993 Brown Plume Study, conducted at the Kintigh power plant, New York, offered coordinated measurements of stack emissions and chemical plume measurements (NO and NO<sub>x</sub> only) to correctly assess the performance of the plume chemistry component of the model near the stack. For the NYSEG cases, the best performance for plume NO<sub>x</sub> concentrations, NO<sub>2</sub>/NO<sub>x</sub> ratios and plume visibility was obtained when the SOC dispersion algorithm was used — better correlations with measurements were noted, and more simulated values were within a factor of two of measured values than with the PGT or FOC dispersion algorithms. These results suggest that the near-stack plume chemistry is correctly simulated when the physical characteristics of the plume are correctly specified.

Seigneur et al. (1999) applied ROME to determine if reductions in SO<sub>2</sub> emissions from specific coal-fired power plants could lead to a discernible change in the wintertime white haze frequently observed in the Dallas-Fort Worth (DFW) urban area. As part of the study, the realism of the plume model simulations was tested by comparing model calculations of plume concentrations with aircraft measurements of SF<sub>6</sub> tracer concentrations (for plume dispersion) and ozone concentrations (for plume chemistry).

As in the studies conducted by Gabruk et al. (1999), Seigneur et al. (1999) found that the performance of the SOC plume dispersion algorithm was better than those of either the PGT or FOC algorithms in explaining observed SF<sub>6</sub> concentrations. The SOC algorithm was able to reproduce the observed plume dilution better than the PGT or FOC algorithms as the plume moved as far as 75 km downwind. Differences between the estimated average concentrations and measured average values increased as a function of downwind distance. The dispersion model used by Lu and Yamada (1998) is based on a SOC formulation.

For the evaluation of the plume chemistry module, Seigneur et al. (1999) focused on the chemistry of the NO/NO<sub>2</sub>/O<sub>3</sub> system because very little SO<sub>2</sub> conversion occurred over the distances and in the dry meteorological conditions in which aircraft measurements of the plume were made. They compared model calculations of the

depletion of ozone concentrations in the plume relative to the background air concentration with ozone concentration depletions measured by the aircraft (determined as the difference between the maximum and minimum O<sub>3</sub> concentrations measured during a plume orbit). The best results were again obtained for the SOC algorithm. Seigneur et al. (1999) concluded that the model captured the salient features of the NO/NO<sub>2</sub>/O<sub>3</sub> plume chemistry, and that differences between model calculations and measurements were primarily due to uncertainties in the plume dispersion calculations rather than in the chemistry calculations.

In addition to the studies described above, the chemical mechanisms used in ROME have been tested in other settings and model frameworks. For example, the CBM-IV mechanism is implemented in the U.S. EPA Urban Airshed Model and has been extensively tested and reviewed. Seigneur and Wegrecki (1990) simulated the chemistry of stratus clouds in the Los Angeles Basin and compared calculated and measured concentrations of sulfite ions, formaldehyde and HMSA in cloud water. The aqueous-phase mechanism used in their study was essentially the same as the one used in ROME. They found that their aqueous-phase chemistry module produced results that were consistent with observations.

## **2.5 Preparation of Model Inputs**

The meteorological data required by ROME consist of plume wind speeds or travel times, as well as vertical profiles of temperature, pressure, relative humidity, and cloud liquid water content. The dispersion data consist of plume widths and vertical profiles of the vertical eddy diffusion coefficients along the plume trajectory. We derived these data from the results of Lu and Yamada (1998) who applied a three-dimensional atmospheric modeling system consisting of a prognostic mesoscale meteorological model (HOTMAC) and a three-dimensional Lagrangian random puff dispersion model (RAPTAD) to simulate the wind, turbulence, and tracer gas concentrations that were observed during the summer intensive period of Project MOHAVE. Section 2.5.1 describes how the HOTMAC/RAPTAD outputs were adapted for our purposes.

Details on the HOTMAC/RAPTAD modeling system can be obtained from Yamada and Bunker (1988) and Lu and Yamada (1998). Lu and Yamada (1998) also conducted a performance evaluation of the modeling system using tracer concentrations measured during Project MOHAVE.

The background chemistry data include concentrations of O<sub>3</sub>, NO<sub>x</sub>, H<sub>2</sub>O<sub>2</sub>, SO<sub>2</sub>, VOCs, PAN, CO, NH<sub>3</sub> and trace metals such as iron and manganese. Whenever possible, we obtained these data from surface and aircraft measurements conducted during the summer intensive period of Project MOHAVE. For chemicals that were not measured during the field study, we reviewed the literature to determine appropriate background concentrations. Section 2.5.2 provides a brief discussion on how background concentrations were selected for our study.

We obtained MPP emissions of SO<sub>2</sub>, NO<sub>x</sub>, and tracer from the Project MOHAVE database. Emissions of trace metals such as iron and manganese (required for the aqueous-phase chemistry calculations) were derived from the SO<sub>2</sub> emissions and ratios of MPP Fe and Mn to SO<sub>2</sub> in the stack obtained from Eatough et al. (1997b). Table 2-1 summarizes these emissions. These emissions were converted to initial puff concentrations for our simulations using the wind speed at the start of the simulation and the initial width of the puff, as well as the thickness of the layer in which the puff was released.

### **2.5.1 Meteorology and dispersion**

ROME has the following input requirements for its transport and dispersion calculations:

- Wind speed as a function of plume travel time at plume height.
- Plume width as a function of plume downwind distance or travel time.
- Vertical eddy diffusivity profiles as a function of plume travel time.

Table 2-1. Emissions from the Mohave Power Plant

<b>Chemical Species</b>	<b>Emission Rate (g/s)</b>
SO <sub>2</sub>	1335
NO <sub>x</sub> (as NO <sub>2</sub> )	720
Fe	2.34
Mn	0.016
OPDCH (tracer)	0.01935

In addition, the following meteorological variables are required for the calculation of chemical kinetic rates as well as the aqueous-phase equilibrium/chemistry computations:

- Vertical profiles of relative humidity, temperature, and pressure as a function of plume travel time.
- Vertical profiles of cloud variables (cloud water content, rain water content, net updraft velocities, net rainfall velocities) as a function of plume travel time.

Most of the above input data were derived from the HOTMAC and RAPTAD outputs of Lu and Yamada (1998), with the exception of some cloud variables such as the net updraft velocities in clouds, or net rainfall velocities. The latter variable was not a critical input for our study, since there were no cases of precipitating clouds during the period of interest. However, cloud updraft velocities were a key input. In keeping with our approach of maximizing ground level concentrations, we specified updraft velocities to be zero in our base case simulations. Sensitivity studies conducted with non-zero updraft velocities resulted in negligible surface concentrations of MPP sulfate.

The HOTMAC/RAPTAD outputs are available at hourly intervals. Many variables are provided in the HOTMAC output files. The HOTMAC results that are relevant for ROME consist of the following:

- gridded, two-dimensional fields of terrain elevations and surface pressure;
- gridded, three-dimensional fields of potential temperature and water vapor mixing ratio, and vertical eddy diffusivities; and
- gridded, three-dimensional fields of cloud water and rain water mixing ratios.

The relevant hourly RAPTAD outputs are:

- puff centroid locations (x,y,z);
- puff  $\sigma_y$ ; and

- puff age counted from release time (this information serves to identify and track the puff).

We used the following procedure to determine the required ROME input variables. Hourly wind speeds at puff height were calculated from the distance traveled by the puff during each time step. Hourly vertical profiles of temperature, relative humidity, pressure, cloud variables, and vertical eddy diffusivities along the puff trajectory were determined using the hourly puff location and the relevant gridded HOTMAC fields. The hourly plume width was defined as  $4 \sigma_y$  since 95% of the plume material is contained within this width.

### **2.5.2 Background concentrations**

Many of the chemicals of interest for our simulations were measured during Project MOHAVE. Data are available from both aircraft measurements and a network of surface monitors. For the period of interest (August 6 to August 16, 1992), aircraft sampling flights were conducted on 3 days (August 5, August 8, and August 12, 1992). Regional as well as plume sampling was performed. We used data from the regional sampling to specify some of our background concentrations. The aircraft data include continuous real-time measurements of  $O_3$ ,  $NO$ ,  $NO_x$  and  $SO_2$ . During sampling, grab samples were also taken and analyzed for speciated VOCs in the laboratory.

Hourly measurements of surface  $H_2O_2$  concentrations were available at only one location (Meadview) in the Grand Canyon. A limited number of sites had hourly observations of surface  $NO_x$  and  $O_3$  concentrations.

We obtained trace metal (iron and manganese) and  $NH_3$  background concentrations from the network of IMPROVE sites. Most of the sites had 24-hour sample durations beginning at 7:00 am daily. Two locations (Hopi Point and Meadview) had 12-hour sample durations. We excluded sites that were in the vicinity of the power plant, such as Dolan Springs and Cottonwood Cove, because these sites may be impacted by the power plant plume relatively often and may not reflect background values.

Table 2-2 presents the ranges of these measured concentrations.

Table 2-2. Range of concentrations measured during August 6 to 16, 1992 in the Project Mohave area

<b>Chemical Species</b>	<b>Concentration</b>
$O_3^{(1,2)}$	35 – 65 ppb
$NO_x^{(1)}$	2 – 8 ppb
$SO_2^{(1,2)}$	0 – 3 ppb
$VOC^{(1,3)}$	24 – 110 ppbC
$CO^{(1)}$	0 to 730 ppb
$NH_3^{(2)}$	0 to 3 ppb
$Fe^{(2)}$	6 to 211 ng/m <sup>3</sup>
$Mn^{(2)}$	0 to 4 ng/m <sup>3</sup>
$H_2O_2^{(2)}$	0 to 4.6 ppb
<p><sup>(1)</sup> Regional (non-plume) aircraft measurements</p> <p><sup>(2)</sup> Regional surface measurements</p> <p><sup>(3)</sup> VOC including methane but excluding oxygenated compounds such as aldehydes</p>	

For the base case simulations, we used the median of the range of measured concentrations for each day of interest to specify the background values. In addition, we used the high and low end of the concentration ranges in additional simulations that we performed to determine chemically-consistent background concentrations for the Grand Canyon region that would maximize the formation of MPP sulfate.

There were no measurements of PAN and aldehydes during Project MOHAVE. Because these species play an important role in influencing SO<sub>2</sub> oxidation rates, it is necessary to specify their background concentrations as accurately as possible. We reviewed the literature for PAN and aldehyde measurements in rural and semi-rural regions and environments similar to the Project MOHAVE region. We also consulted with Dr. Daniel Grosjean, an expert in PAN and aldehyde measurements, to determine appropriate background concentrations to use in our simulations.

Table 2-3a summarizes the range of PAN concentrations measured at a number of locations as well as the baseline value recommended by Grosjean (1997). Table 2-3b provides the same information for formaldehyde and acetaldehyde concentrations. We used the recommended values of Grosjean (1997) for our base case simulations.

Table 2-3a. PAN concentrations measured at a number of locations

<b>Source</b>	<b>Concentration</b>	<b>Location/Period</b>
Gaffney et al., 1993	0.03 - 0.8 ppb	SW U.S. (August 1988)
Fahey et al., 1986	0.1 - 0.8 ppb (hourly averages of 23 days, max. hourly = 2.3 ppb)	SW U.S. (Summer 1984)
Spicer et al., 1983	0.5 ppb Regional background: 0.1 - 0.3 ppb	NE U.S. (July-August 1981)
Hartsell et al., 1994	0 - 1.2 ppb	NE U.S. (June-July 1992)
Roberts et al., 1995	0.3 - 0.8 ppb	Eastern North America (July-August 1988)
Grosjean, 1997 (Personal communication)	Baseline PAN: 0.25 ppb	Value selected for summer for Project MOHAVE region

Table 2-3b. Formaldehyde and acetaldehyde concentrations measured at a number of locations

<b>Source</b>	<b>Concentration</b>	<b>Location/Period</b>
Dawson & Farmer, 1988	HCHO: 0.25 - 1.9 ppb < 1 ppb at 3 sites	4 sites in SW U.S. (Summer 1980, 1981)
Altshuller, 1983	HCHO: 0.1 - 0.8 ppb	SW U.S. (July - August 1981)
Schulam et al., 1985	CH <sub>3</sub> CHO: 0.2 - 0.8 ppb	NE U.S. (August 1983)
Grosjean, 1991	$\frac{\text{CH}_3\text{CHO}}{\text{HCHO}} = 0.5 - 0.8$	Southern California (Sept. 1988 - Sept. 1989)
Tanner & Meng, 1984	$\frac{\text{CH}_3\text{CHO}}{\text{HCHO}} \sim 0.5$	NE U.S. (Summer 1982)
Grosjean, 1997 (Personal Communication)	Baseline HCHO: 0.5 ppb Baseline CH <sub>3</sub> CHO: 0.25 ppb	Value selected for summer for Project MOHAVE region

### 3. BASE CASE SIMULATIONS

For the base case simulations, we used puff trajectories arriving from MPP and traveling in the general direction of Meadview or Hopi Point, two receptor sites of interest in the Grand Canyon. Meadview is located at the western boundary of Grand Canyon National Park at about 100 km NNE of MPP, while Hopi Point is located on the south rim of the Grand Canyon, at about 280 km NE of MPP.

During the summer period of 1992, Meadview was frequently impacted by flow from MPP, as shown by tracer measurements (e.g., Pitchford et al., 1997; Green and Tombach, 1997). In particular, elevated concentrations of MPP tracer were measured at Meadview during most of the 11 day period of August 6 to August 16, 1992. In contrast, tracer measurements at Hopi Point showed infrequent impact of the MPP plume. These observations are consistent with the puff trajectory information developed by Lu and Yamada (1998) — approximately 50% of the puffs released in their simulation influenced Meadview, but less than 4% influenced Hopi Point. In our analysis, a puff is assumed to influence a receptor if it arrives within  $2\sigma_y$  of the receptor.

#### 3.1 Selection of Trajectories

Lu and Yamada (1998) simulated more than 2000 puffs over a period of a little more than 12 days (early morning of August 5, 1992 to late morning of August 17, 1992). Over 1000 puffs influenced Meadview, and 75 puffs influenced Hopi Point. Many of the puff trajectories had durations of over 20 hours. Because it was neither practical nor necessary to simulate the chemistry of all these puffs with ROME, we selected a sample of the trajectories for our study. The criteria used to select puff trajectories for our simulations are listed below.

- **MPP tracer concentrations:** During the period of interest (August 6 to August 16, 1992), MPP tracer concentrations ranged from 0.11 to 5.89 femtoliters per liter (fL/L) at Meadview and 0.07 to 0.87 at Hopi Point. We first selected days on which high tracer concentrations were measured.

- **Presence of clouds:** We attempted to select all days on which there was extensive cloud cover and cloud bases were low for at least part of the puff trajectories. We used the cloud water contents provided by Lu and Yamada (1998) to diagnose the presence and extent of clouds. A cut-off level of 0.01 g/m<sup>3</sup> cloud water content was used (i.e., only gas-phase chemistry was simulated if the cloud water content was less than 0.01 g/m<sup>3</sup>). While this level is low (e.g., a typical value for cloud water content in a stratus cloud is 0.1 g/m<sup>3</sup>), it allowed us to maximize the possible conversion of MPP SO<sub>2</sub> to sulfate. As it turned out, high cloud cover and low cloud bases were predicted by Lu and Yamada (1998) only for the night of August 5 and morning of August 6. We selected all trajectories for August 5 and 6 that influenced Meadview or Hopi Point and that had some potential for interacting with clouds.
- **Distance to receptors:** We selected puffs that came closest to the two receptors.
- **Puff widths:** We attempted to select puffs with a wide range (24 km to 120 km) of plume widths to allow for different dilution histories.

After the trajectories were selected, we developed the initial conditions, background chemistry and meteorological data files required for the simulation of these trajectories with ROME using the procedures described in Section 2. Table 3-1 summarizes the background concentrations for the base case simulations for the 3 days during the period when aircraft data were available. Note that Table 3-1 shows the total VOC concentrations in ppbC, obtained by summing the product of the concentrations of individual VOC species in the CBM-IV mechanism, including formaldehyde and higher aldehydes, and their carbon numbers.

We then performed the transport/chemistry calculations for these trajectories using ROME. The instantaneous puff concentrations estimated by ROME were converted to 12-hour average concentrations at the receptor location. The 12-hour average modeled and observed tracer concentrations were compared to determine scaling factors for the modeled 12-hour average sulfate concentrations.

Table 3-1. Background concentrations (in ppb unless otherwise indicated) for the base case simulations

<b>Species</b>	<b>August 5-7, 1992</b>	<b>August 8-9, 1992</b>	<b>August 13-16, 1992</b>
O <sub>3</sub>	50	45	50
NO <sub>2</sub>	4	3	3
H <sub>2</sub> O <sub>2</sub>	1.34	1.34	2.3
SO <sub>2</sub>	1	1	1
VOC (ppbC)	28.4	28.9	18.9
PAN	0.25	0.25	0.25
CO	89	97	44
NH <sub>3</sub>	0.3	0.3	0.3
Fe (ng/m <sup>3</sup> )	34	34	34
Mn (ng/m <sup>3</sup> )	1	1	1

The following section describes the trajectories selected for our base case analysis.

### 3.2 Description of Trajectories

A total of 13 puff trajectories were selected to simulate the transport and chemistry of MPP releases arriving at Meadview, and 10 trajectories were selected to investigate MPP impacts at Hopi Point. We found that there were no common trajectories, i.e., puffs traveling to Meadview did not travel to Hopi Point and puffs arriving at Hopi Point did not pass through Meadview.

The highest 12-hour average MPP tracer concentration at Meadview was measured during the period from 7 p.m. on August 13 to 7 a.m. on August 14, 1992. High tracer concentrations were also measured during the 12-hour periods from 7 p.m. on August 8 to 7 a.m. on August 9 and from 7 a.m. to 7 p.m. on August 9. We used these three periods for the initial selection of trajectories. In addition, as discussed in Section 3.1, low cloud bases were diagnosed on the night of August 5 and the morning of August 6. We selected trajectories going to Meadview that interacted with clouds on these days.

Many of the 13 trajectories selected for Meadview, particularly during the latter portion of the study period, impacted the receptor during more than one 12-hour averaging period. For these trajectories, we calculated concentrations for each 12-hour period impacted, even if high tracer concentrations were not measured during the period.

Table 3-2 provides a summary of the trajectory data for trajectories going from MPP to Meadview. The trajectory number in the table corresponds to the puff release number from the results of Lu and Yamada (1998), i.e., trajectory number 123 corresponds to the 123rd puff released in their simulation. The table provides the release time of the puff, the time at which it first impacts the receptor (i.e., arrives within a distance of  $2\sigma_y$  of the receptor), the residence time (i.e., the total number of hours for which it impacts the receptor), the total travel time (i.e., the time from release to the final time at which it impacts the receptor, which is relevant to plume chemical transformations), the 12-hour averaging periods during which it impacts the receptor (where the night period refers to the 12-hour period from 7 p.m. of the current day to 7

Table 3-2. Description of selected trajectories traveling from the Mohave Power Plant to Meadview.

Trajectory Number	Release Time	First Contact Time <sup>1</sup>	Last Contact Time <sup>1</sup>	Residence Time <sup>2,3</sup> (h)	Travel Time <sup>4</sup> (h)	Affected 12-hr Period <sup>5</sup>	Mean Wind Speed (m/s)	Cloud Interaction	Lowest Cloud Base (m agl)
123	8/5 10:00 p.m.	8/6 6:00 a.m.	8/6 6:00 a.m.	1	8	8/5 Night	5.0	Yes	200
129	8/5 11:00 p.m.	8/6 9:00 a.m.	8/6 9:00 a.m.	1	10	8/6 Day	3.7	Yes	0
173	8/6 6:00 a.m.	8/6 5:00 p.m.	8/7 12:00 a.m.	8	18	8/6 Day 8/6 Night	2.9	No	1500
156	8/6 3:00 a.m.	8/6 5:00 p.m.	8/6 10:00 p.m.	6	19	8/6 Day 8/6 Night	2.7	No	1000
245	8/6 4:00 p.m.	8/7 1:00 a.m.	8/7 3:00 a.m.	3	11	8/6 Night	3.5	No	1500
572	8/8 4:00 p.m.	8/9 1:00 a.m.	8/9 12:00 p.m.	11	20	8/8 Night 8/9 Day	2.7	No	2000
593	8/8 7:00 p.m.	8/9 4:00 a.m.	8/9 10:00 a.m.	7	15	8/8 Night 8/9 Day	3.3	No	No Clouds
1350	8/13 10:00 a.m.	8/13 7:00 p.m.	8/14 8:00 a.m.	14	22	8/13 Day 8/13 Night 8/14 Day	2.7	Some	1000
1366	8/13 12:00 p.m.	8/14 5:00 a.m.	8/14 10:00 p.m.	17	34	8/13 Night 8/14 Day 8/14 Night	2.6	No	1500
1387	8/13 3:00 p.m.	8/14 2:00 a.m.	8/14 9:00 p.m.	20	30	8/13 Night 8/14 Day 8/14 Night	2.5	No	1500
1409	8/13 6:00 p.m.	8/14 4:00 a.m.	8/15 12:00 a.m.	21	30	8/13 Night 8/14 Day 8/14 Night	2.5	No	1500
1653	8/15 6:00 a.m.	8/16 12:00 a.m.	8/16 3:00 a.m.	4	21	8/15 Night	3.5	No	2000
1756	8/15 9:00 p.m.	8/16 4:00 a.m.	8/16 11:00 a.m.	8	14	8/15 Night 8/16 Day	3.1	No	2000

<sup>1</sup> The first contact time indicates the time at which the puff first arrives within  $2\sigma_y$  of Meadview. The last contact time indicates the last time at which the puff is within  $2\sigma_y$  of Meadview.

<sup>2,3</sup> The residence time represents the total hours during which the puff persistently stayed at Meadview within a distance less than  $2\sigma_y$ . It is calculated as follows:  
For a consecutive stay episode (e.g., trajectory #173, #156, #123, #129, #245, #593, #1350, #1387, #1409, #1653, and #1750):

Residence time = the last contact time - the first contact time

For a non-consecutive stay episode (e.g., trajectory #572 and #1366):

Residence time = the last contact time - the first contact time - the number of hours during which the distance of the puff from Meadview was more than  $2\sigma_y$ .

<sup>4</sup> The travel time indicates the sum of the travel time of each trajectory from the Mohave power plant to Meadview and its residence time at Meadview.

<sup>5</sup> The 12-hour period represents the period during which the observations were made. The night period indicates the 12 hours between 7:00 p.m. of the current day to 7:00 a.m. of the next day, and the day period indicates the 12 hours between 7:00 a.m. to 7:00 p.m. of the current day.

a.m. of the next day shown in the table, and the day period refers to the 12-hour period from 7 a.m. to 7 p.m. of the day shown in the table). The table also provides the average wind speed for the total duration of the trajectory and information on interaction of the puff with clouds, and the lowest cloud base during the trajectory.

As shown in Table 3-2, trajectories 123 and 129 had some interaction with clouds. These trajectories also had the smallest travel times and residence times of all the trajectories simulated. Clouds were diagnosed in Layer 1 of the model (i.e., cloud base was zero) for part of the duration of trajectory 129. Thus, this trajectory had the largest potential for forming sulfate from aqueous-phase chemistry.

Trajectories 1366, 1387, and 1409 had the longest residence and travel times and the smallest mean wind speeds. These trajectories impacted Meadview for 3 separate 12-hour averaging periods —the night of August 13 and the day and night of August 14. These trajectories had negligible interaction with clouds, since there were no clouds below 1500 m.

Table 3-3 provides a similar summary for trajectories going from MPP to Hopi Point. We selected 10 trajectories for the Hopi Point simulations. None of the trajectories going to Hopi Point had any significant interaction with clouds.

### **3.3 Results**

Table 3-4 summarizes the base case results for Meadview. The table shows the model estimates of sulfate concentrations attributable to MPP that were calculated for each 12-hour averaging period from the 13 trajectories simulated for Meadview. The residence time of the puffs at Meadview was taken into account in those calculations. The puff sulfate concentration used was that at the location of Meadview. The measured 12-hour average sulfate concentrations for each period and the relative contribution of MPP to the measured sulfate are also provided. In addition, an aggregate MPP sulfate to MPP SO<sub>2</sub> ratio at Meadview is provided — this is an approximate measure of the conversion of MPP SO<sub>2</sub> to sulfate. It is an approximation because SO<sub>2</sub> and sulfate are deposited at different rates along the puff trajectory.

Table 3-3. Description of selected trajectories traveling from the Mohave Power Plant to Hopi Point

Trajectory Number	Release Time	First Contact Time <sup>1</sup>	Last Contact Time <sup>1</sup>	Residence Time <sup>2</sup> (h)	Travel Time <sup>3</sup> (h)	Affected 12-hr Period <sup>4</sup>	Mean Wind Speed (m/s)	Cloud Interaction	Lowest Cloud Base (m agl)
165	8/6 4:00 p.m.	8/7 9:00 a.m.	8/7 12:00 p.m.	4	32	8/7 Day	2.8	No	700
176	8/6 6:00 a.m.	8/7 12:00 a.m.	8/7 1:00 a.m.	2	19	8/6 Night	4.0	No	1000
210	8/6 11:00 a.m.	8/7 4:00 a.m.	8/7 5:00 a.m.	2	18	8/6 Night	3.9	No	1000
223	8/6 1:00 p.m.	8/7 8:00 a.m.	8/7 9:00 a.m.	2	20	8/7 Day	3.7	No	700
500	8/8 5:00 a.m.	8/9 6:00 p.m.	8/9 11:00 p.m.	6	42	8/9 Day 8/9 Night	2.7	No	2500
508	8/8 7:00 a.m.	8/9 1:00 a.m.	8/10 3:00 a.m.	15	44	8/9 Day 8/9 Night	2.5	No	2000
1479	8/14 4:00 a.m.	8/16 12:00 a.m.	8/16 5:00 a.m.	6	49	8/15 Night	2.3	No	2000
No	8/15 5:00 a.m.	8/16 10:00 a.m.	8/16 3:00 p.m.	6	34	8/15 Night 8/16 Day	3.2	No	2000
1693	8/15 12:00 p.m.	8/16 10:00 a.m.	8/16 12:00 p.m.	3	24	8/16 Day	4.0	No	2000
1750	8/15 8:00 p.m.	8/16 6:00 p.m.	8/16 7:00 p.m.	2	23	8/16 Day	4.0	No	2000

<sup>1</sup> The first contact time indicates the time at which the puff first arrives within  $2\sigma_y$  of Hopi Point. The last contact time indicates the last time at which the puff is within  $2\sigma_y$  of Hopi Point.

<sup>2</sup> The residence time represents the total hours during which the puff persistently stayed at Hopi Point within a distance less than  $2\sigma_y$ . The residence time is calculated as follows:

Residence time = the last contact time - the first contact time

<sup>3</sup> The travel time indicates the sum of the travel time of each trajectory from the Mohave power plant to Hopi Point and its residence time at Hopi Point.

<sup>4</sup> The 12-hour period represents the period during which the observations were made. The night period indicates the 12 hours between 7:00 p.m. of the current day to 7:00 a.m. of the next day, and the day period indicates the 12 hours between 7:00 a.m. to 7:00 p.m. of the current day.

Table 3-4. Base case results for Meadview

<b>Date of initial time</b>	<b>12-hour period</b>	<b>MPP Sulfate (ng/m<sup>3</sup>)</b>	<b><u>Sulfate</u> (%)SO<sub>2</sub></b>	<b>Observed Sulfate (ng/m<sup>3</sup>)</b>	<b>Calculated MPP contribution to observed sulfate (%)</b>
8/5/92	7p.m. - 7a.m.	22	1	1636	1.3
8/6/92	7a.m. - 7p.m.	123	18	2673	4.6
8/6/92	7p.m. - 7a.m.	31	3	2918	1.1
8/8/92	7p.m. - 7a.m.	8	< 1	1645	< 1.0
8/9/92	7a.m. - 7p.m.	90	5	2043	4.4
8/13/92	7a.m. - 7p.m.	10	3	1347	< 1.0
8/13/92	7p.m. - 7a.m.	92	2	1791	5.1
8/14/92	7a.m. - 7p.m.	244	14	2891	8.4
8/14/92	7p.m. - 7a.m.	382	30	2037	18.8
8/15/92	7p.m. - 7a.m.	190	13	2514	7.5
8/16/92	7a.m. - 7p.m.	53	8	2427	2.2

As shown in Table 3-4, the estimated contribution of MPP to 12-hour average sulfate concentrations measured at Meadview ranges from less than 1% to 18.4% for the base case simulations. Over the entire period, the estimated average MPP contribution to 12-hour average sulfate concentrations is approximately 5%. Modeled MPP 12-hour average sulfate concentrations range from less than 10 ng/m<sup>3</sup> to 382 ng/m<sup>3</sup>, with an average value of approximately 113 ng/m<sup>3</sup>. The MPP sulfate to MPP SO<sub>2</sub> ratio ranges from less than 1% to 30%. The average ratio over the period is approximately 9%.

The highest MPP 12-hour average sulfate concentration of 374 ng/m<sup>3</sup> is predicted for the period from 7 p.m. August 14 to 7 a.m. August 15. This is also the largest contribution of MPP (18.8%) to the total sulfate concentration measured at Meadview. As shown in Table 3-2, three puffs (1366, 1387, and 1409) impacted Meadview during this 12-hour period. All three puffs were released at various times on August 13 and had long residence and transport times, allowing time for conversion of MPP SO<sub>2</sub> to sulfate, particularly on August 14. As shown by the ratio of MPP sulfate to SO<sub>2</sub> for this period in Table 3-4, the largest conversion of MPP SO<sub>2</sub> to sulfate is associated with these three puffs.

The second highest MPP 12-hour average sulfate concentration at Meadview (244 ng/m<sup>3</sup>), which is also the second largest contribution of MPP (8.4%) to sulfate concentrations at Meadview, is predicted for the period from 7 a.m. August 14 to 7 p.m. August 14. Most of this contribution is associated with the same puffs (1366, 1387, and 1409) that produced the highest MPP sulfate concentration on the night of August 14, 1992.

It is important to note that the highest calculated sulfate concentrations occur for dry periods (i.e., no interaction of the plume with clouds) with low wind speeds. The period when the plume interacts with clouds (August 5 to 6, 1992) leads to lower sulfate concentrations because the frequency of plume impacts at Meadview is low.

The base case results for Hopi Point are summarized in Table 3-5. In general, MPP sulfate concentrations are smaller at Hopi Point than at Meadview. The estimated MPP contribution to observed 12-hour average sulfate concentrations at Hopi Point ranges from less than 1% to 6.4%. The average contribution over the period is approximately 3.5%. Modeled 12-hour average MPP sulfate concentrations range from

Table 3-5. Base case results for Hopi Point

<b>Date of initial time</b>	<b>12-hour period</b>	<b>MPP Sulfate (ng/m<sup>3</sup>)</b>	<b><u>Sulfate</u> (%) SO<sub>2</sub></b>	<b>Observed Sulfate (ng/m<sup>3</sup>)</b>	<b>MPP Contribution (%)</b>
8/6/92	7p.m. - 7a.m.	2	13	1217	< 1.0
8/7/92	7a.m. - 7p.m.	17	15	1799	< 1.0
8/9/92	7a.m. - 7p.m.	96	37	1572	6.0
8/9/92	7p.m. - 7a.m.	28	39	1648	1.7
8/15/92	7p.m. - 7a.m.	64	37	1322	4.8
8/16/92	7a.m. - 7p.m.	129	29	2014	6.4

less than  $10 \text{ ng/m}^3$  to  $129 \text{ ng/m}^3$ , with an average value of  $56 \text{ ng/m}^3$ , about 50% of the average MPP sulfate at Meadview.

In contrast, the ratio of MPP sulfate to MPP  $\text{SO}_2$  at Hopi Point is generally larger than the corresponding value for Meadview, primarily due to the larger travel times associated with transport from MPP to Hopi Point. The ratios range from 13% to 39%, with an average value of 28%, about 3 times the average ratio of 9% for Meadview.

The highest MPP 12-hour average sulfate concentration of  $129 \text{ ng/m}^3$  at Hopi Point is calculated for the period from 7 a.m. August 16 to 7 p.m. August 16. This concentration is about a factor of 3 lower than the highest estimated MPP 12-hour average sulfate concentration at Meadview ( $382 \text{ ng/m}^3$ ). This is also the largest contribution of MPP (6.4%) to the total 12-hour average sulfate concentration measured at Hopi Point, less than half of the largest contribution (18.8%) at Meadview.

The second highest estimated MPP 12-hour average sulfate concentration at Hopi Point ( $94 \text{ ng/m}^3$ ) for the period from 7 a.m. August 9 to 7 p.m. August 9 also corresponds to the second largest contribution of MPP (6%) to sulfate concentrations at Hopi Point. The second highest estimated 12-hour average MPP sulfate concentration at Hopi Point is about 60% lower than the corresponding value at Meadview. The second highest MPP sulfate contribution at Hopi Point is about 33% lower than the second highest MPP contribution at Meadview.

While the results presented above provide an estimate of the range of expected MPP contributions for the base case conditions assumed in our study, it is of interest to investigate the range of plausible MPP contributions for a variety of conditions. In the following section, we present results from additional studies including studies that were designed to estimate the maximum contribution of MPP to sulfate concentrations in the Grand Canyon region.

## 4. ADDITIONAL STUDIES

We performed several additional calculations to examine the impact of MPP for a number of hypothetical and/or plausible scenarios. Some of these calculations involved additional simulations with ROME, while others used previous simulation results to draw inferences. In this section, we present results from these analyses.

### 4.1 Effect of MPP NO<sub>x</sub> Emissions

As discussed in Section 2.2, gas-phase SO<sub>2</sub> oxidation rates in a power plant plume are significantly lower than background oxidation rates, particularly near the stack, because the NO<sub>x</sub> in the plume scavenges O<sub>3</sub> and OH radicals. Aqueous-phase oxidation rates may also be influenced, particularly when H<sub>2</sub>O<sub>2</sub> concentrations are low, because the nitric acid formed in the plume will reduce the cloud pH, thereby reducing oxidation rates of SO<sub>2</sub> by O<sub>3</sub> and O<sub>2</sub> (in the presence of trace metals such as iron and manganese). However, the largest effects are expected to be on the gas-phase oxidation rates.

To illustrate this, Figure 4-1 shows the ratio of the plume SO<sub>2</sub> gas-phase oxidation rate to the ambient rate as a function of plume SO<sub>2</sub> concentrations. The simulation was performed for August 6, 1992. Near the stack, when plume SO<sub>2</sub> concentrations (and plume NO<sub>x</sub> concentrations) are high, the plume SO<sub>2</sub> oxidation rates are a factor of 10 smaller than ambient oxidation rates. Plume oxidation rates approach ambient rates as the plume gets diluted.

To examine the effect of MPP NO<sub>x</sub> emissions on plume SO<sub>2</sub> oxidation rates and the formation of sulfate in the plume, we performed hypothetical studies in which MPP NO<sub>x</sub> emissions were set to zero. The effect of this scenario was investigated for two 12-hour measurement periods at Meadview. The first period corresponded to the night of August 5, and the second period corresponded to the night of August 14.

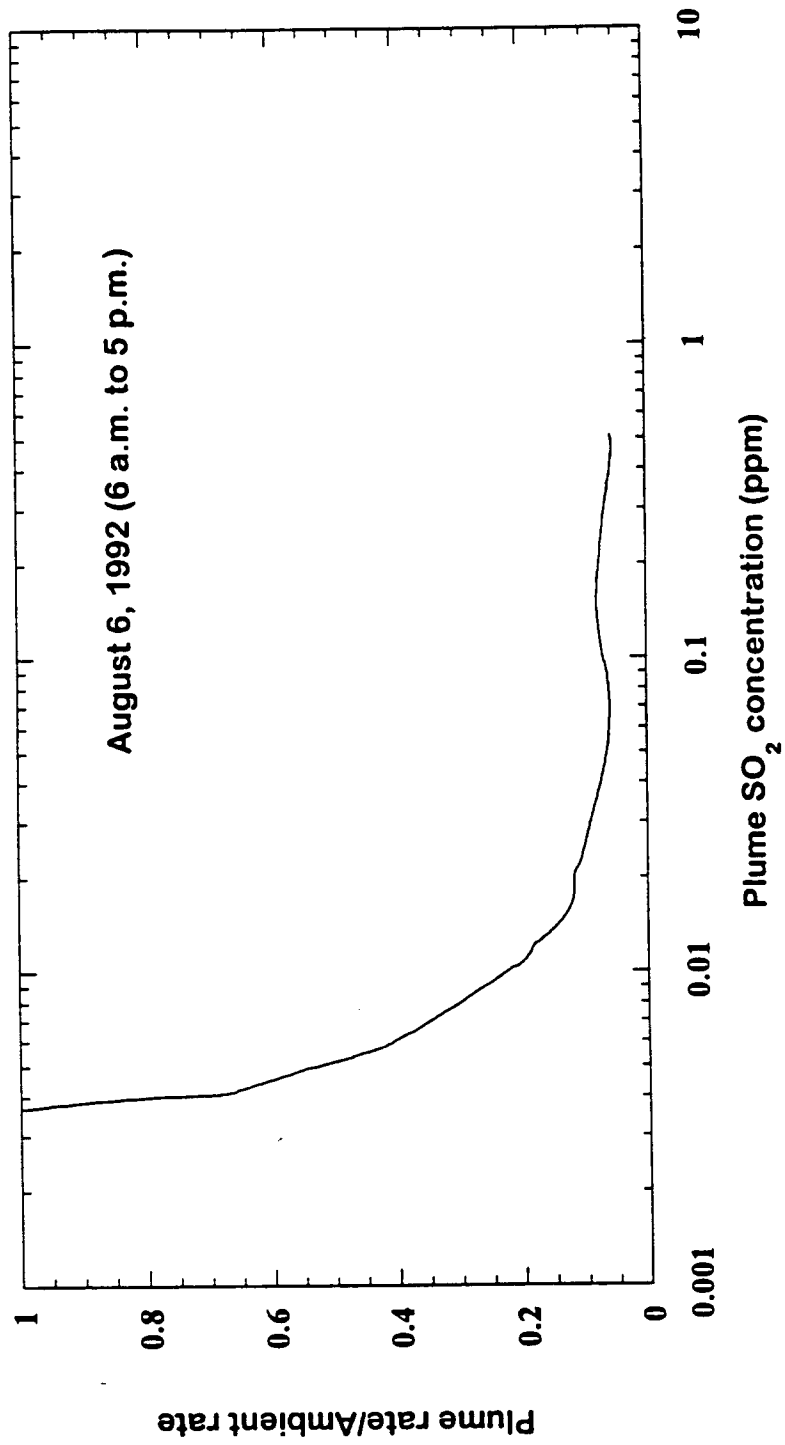


Figure 4-1. The ratio of the plume SO<sub>2</sub> gas-phase oxidation rate to the ambient rate as a function of plume SO<sub>2</sub> concentration.

For the night of August 5, the increase in MPP sulfate concentrations with the elimination of  $\text{NO}_x$  in the plume is small (~10%). As shown previously in Table 3-2, only one trajectory was simulated for this 12-hour period. This trajectory (trajectory 123) was released at 10:00 p.m. on August 5 and arrived at Meadview at 6:00 a.m. on August 6. Thus, the gas-phase conversion of  $\text{SO}_2$  for this night-time only trajectory was negligible, and any sulfate formed in the plume came primarily from the aqueous-phase oxidation of  $\text{SO}_2$ . Thus, the effect of MPP  $\text{NO}_x$  emissions on  $\text{SO}_2$  oxidation rates for this trajectory is expected to be small.

For the night of August 14, setting MPP  $\text{NO}_x$  emissions to zero results in a 24% increase in MPP sulfate concentrations as compared to the base case results. While this increase is significant, it is not as dramatic as might be expected from our earlier discussion. To explain this, recall from the discussion in Section 3.3 that the three trajectories impacting Meadview during this 12-hour period had long residence and transport times (the average transport time for the 3 trajectories was about 31 hours). Thus, even though plume  $\text{SO}_2$  oxidation rates were suppressed by  $\text{NO}_x$  during the first day of transport (August 13) in the base case simulations, the plumes were dilute enough during the daytime of August 14 for the influence of  $\text{NO}_x$  to become less important. This is illustrated in Figure 4-2, which shows the ratio of the instantaneous sulfate concentration for the case when MPP  $\text{NO}_x$  is set to zero to the base case value as a function of time for a puff released on August 13. We see that, near the stack, the amount of sulfate formed in the plume when MPP  $\text{NO}_x$  emissions are set to zero is more than a factor of 10 larger than in the base case. As the plume gets diluted, the effect of initial  $\text{NO}_x$  in the plume becomes small.

## 4.2 Effect of Overlapping Puffs

Overlapping puffs can cause a reduction in plume  $\text{SO}_2$  oxidation rates by creating a more concentrated plume — the higher  $\text{NO}_x$  concentrations in the plume will primarily reduce gas-phase oxidation rates (near the stack), and the higher plume  $\text{SO}_2$  concentrations will reduce the relative amount of  $\text{H}_2\text{O}_2$  available for aqueous-phase oxidation.

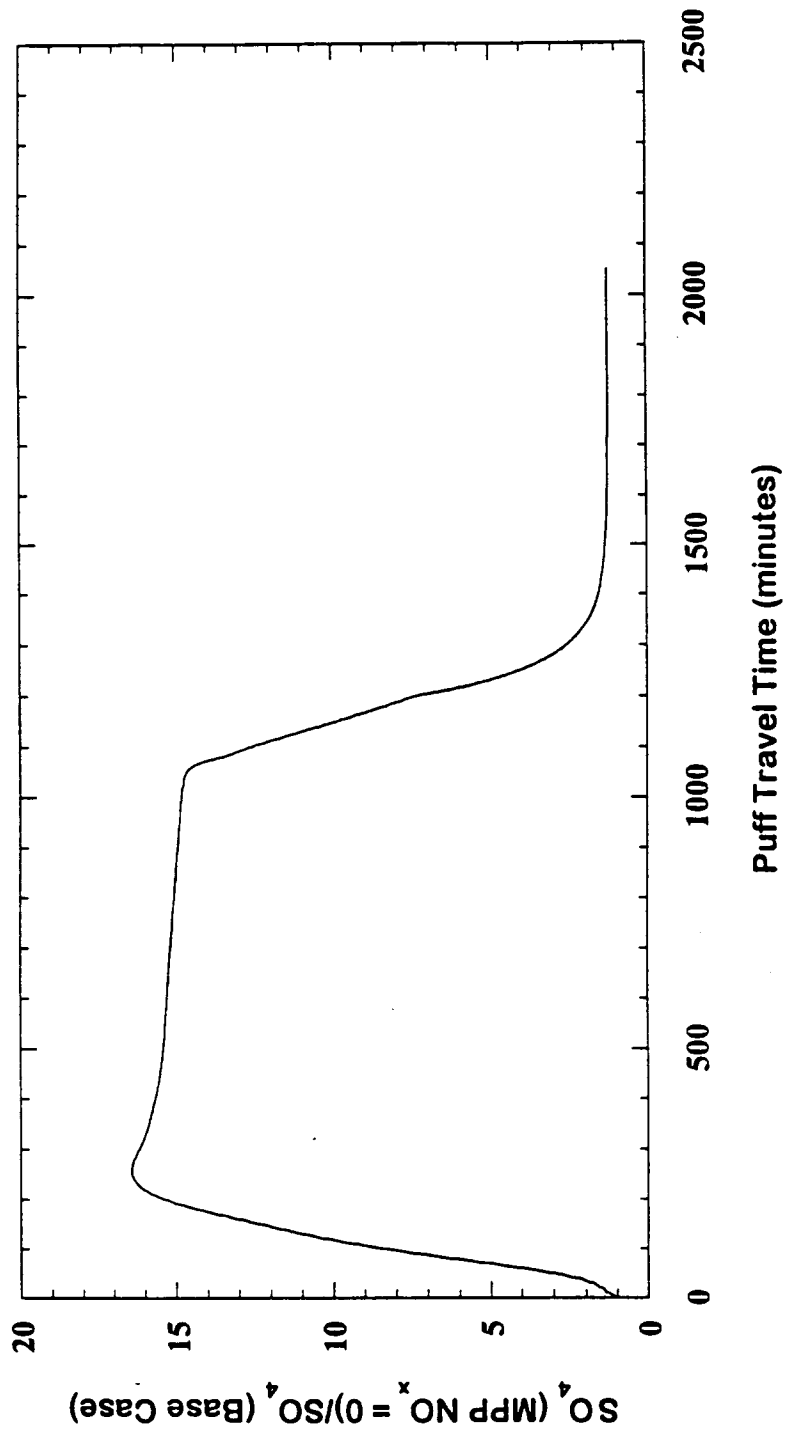


Figure 4-2. The ratio of the instantaneous sulfate concentration in the plume when  $MPP\ NO_x = 0$  to the base case value as a function of travel time.

Although ROME does not treat the merging and overlapping of separate plumes, the overlapping effect can be approximately simulated by combining two puffs and releasing them simultaneously. In other words, the initial concentrations in the puffs are doubled and the simulation is performed. However, to ensure that this does not result in a doubling of total material emitted from the stack, concentrations at the receptor are halved. Thus, the plume material reaching the receptor remains the same for an inert tracer but plume chemistry differs due to higher plume concentrations. We performed these hypothetical simulations for the same 12-hour periods discussed in Section 4.1.

For the 12-hour measurement period from 7 p.m. August 5 to 7 a.m. August 6, concentrating the plume results in a net reduction of 47% in MPP sulfate at Meadview. Recall that for this period, the sulfate in the plume is formed primarily from aqueous-phase oxidation. Because the oxidation is limited by the availability of  $\text{H}_2\text{O}_2$ , the amount of sulfate formed by doubling the initial  $\text{SO}_2$  concentration is nearly unchanged from the base case value. When the sulfate concentration is halved to account for the fact that actual emissions were not doubled, the concentration at Meadview is reduced by almost a factor of 2.

On the other hand, for the 12-hour measurement period on the night of August 14, doubling the initial plume concentrations nearly doubles the amount of sulfate formed. When the sulfate concentration is halved to reflect the actual emissions, the concentration at Meadview is almost unchanged from the base case value. Thus, doubling the  $\text{NO}_x$  concentration in the plume does not have any effect on plume  $\text{SO}_2$  oxidation rates. This result is in contrast to the result obtained when  $\text{NO}_x$  concentrations in the plume are set to zero (see Section 4.1). This suggests that increasing  $\text{NO}_x$  concentrations in the plume beyond a certain value may have a negligible effect, at least for this particular case. To confirm this, we performed sensitivity simulations for puff 1366 in which we set the initial  $\text{NO}_x$  in the plume to 50% and 150% of the base case value. Figure 4-3 shows the ratio of the instantaneous sulfate concentration for the perturbation in  $\text{NO}_x$  emission to the base case value as a function of puff travel time. We see that, as the initial  $\text{NO}_x$  in the plume is increased, sulfate formation rates near the stack are suppressed. However, the

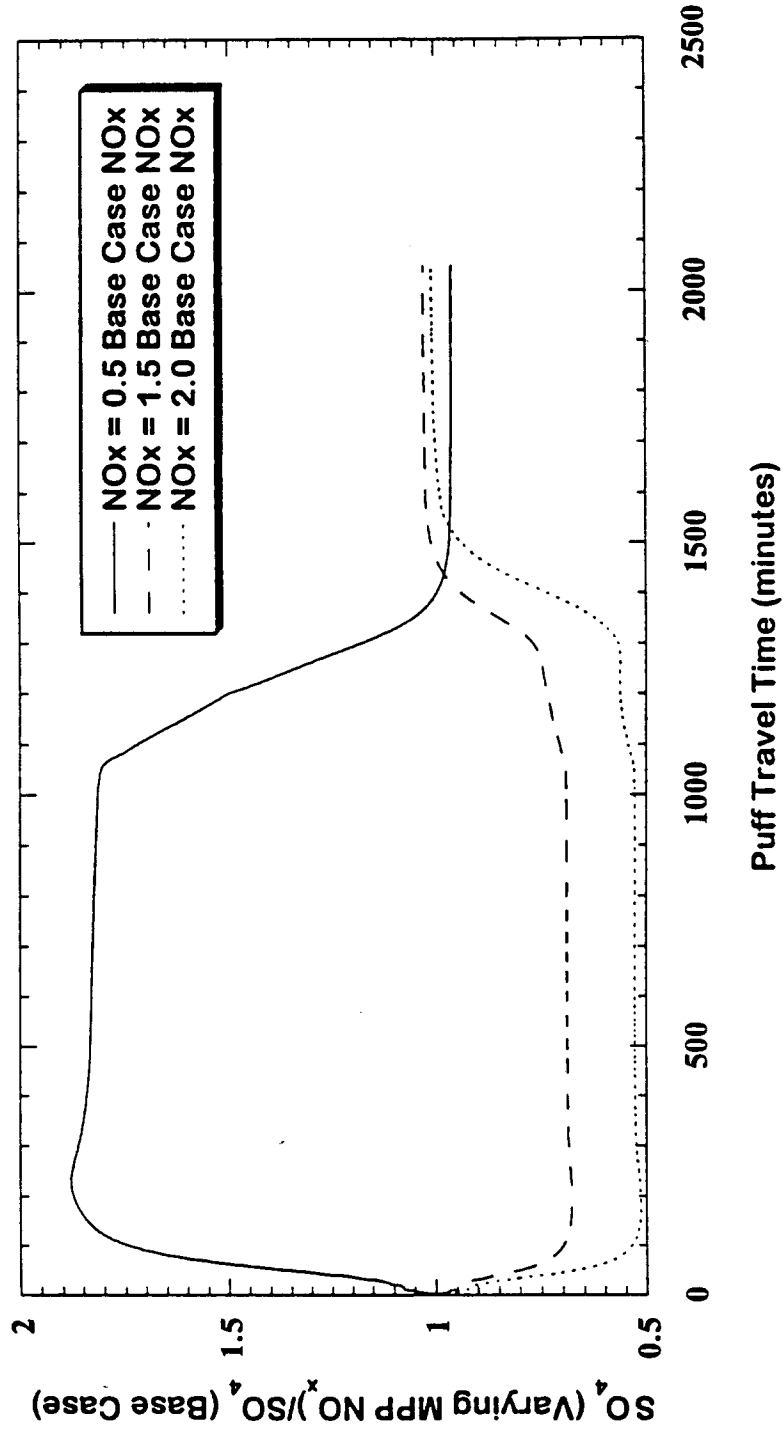


Figure 4-3. The ratio of the instantaneous sulfate concentration in the plume for different MPP NO<sub>x</sub> values to the base case value as a function of travel time.

effect of increased NO<sub>x</sub> emissions levels off after a certain point, and there is no discernible difference between the cases when NO<sub>x</sub> is 150% and 200% of the base case value.

### **4.3 Effect of 90% Reduction in MPP SO<sub>2</sub> Emissions**

These hypothetical studies were performed to determine the change in MPP sulfate concentrations at Meadview for a given change in SO<sub>2</sub> emissions. The simulations were conducted for two puffs (puffs 123 and 129) that interacted with clouds, since SO<sub>2</sub> conversion in all the other puffs was primarily due to gas-phase processes and the response was expected to be linear for these other puffs.

Puff 123 was the only one impacting Meadview during the 12-hour period from 7 p.m. August 5 to 7 a.m. August 6. Decreasing MPP SO<sub>2</sub> emissions by 90% resulted in only a 11% reduction in MPP sulfate at Meadview, illustrating the highly non-linear nature of aqueous-phase SO<sub>2</sub> oxidation.

For the 12-hour period from 7 a.m. August 6 to 7 p.m. August 6, there were three puffs (puffs 129, 156 and 173) impacting Meadview. Of these puffs, only puff 129 had significant aqueous-phase conversion of SO<sub>2</sub>. We performed the SO<sub>2</sub> emission reduction study for this puff. For the other two puffs, we assumed that the response to the MPP SO<sub>2</sub> reduction was linear, i.e., MPP sulfate from the two puffs was 10% of the base case values. The overall reduction in 12-hour average MPP sulfate concentrations due to the reduction in SO<sub>2</sub> emissions was predicted to be 81%. Thus, the response was only slightly non-linear, because the two puffs that involved only gas-phase conversion contributed to the majority (85%) of sulfate concentration for the base case.

### **4.4 Effect of Las Vegas Urban Plume**

One of the issues of interest to the Project MOHAVE study is the contribution of the Las Vegas plume to visibility degradation in the Grand Canyon region. While the study of this issue is a project by itself, we attempted to make an estimate of the contribution using the data at our disposal. We were provided puff trajectory data for

puff releases from Las Vegas from the RAPTAD simulations of Lu and Yamada (1998). Using these data and the procedure described in Section 2.5.1, we developed meteorological and puff trajectory information for Las Vegas releases traveling to Meadview and Hopi Point. There were only 6 trajectories that approached Meadview within  $2\sigma_y$  and no trajectories that reached Hopi Point.

We simulated all 6 puff trajectories that approached Meadview using ROME. Background chemical concentrations and initial VOC and  $\text{NO}_x$  concentrations in the plume were chosen to be representative of the Las Vegas region, based on aircraft measurements taken in the region. We assumed that Las Vegas  $\text{SO}_2$  emissions were a factor of 10 lower than MPP  $\text{SO}_2$  emissions (Pitchford, 1997).

The results from this exercise showed that the Las Vegas urban plume had a negligible contribution on sulfate concentrations at Meadview (less than 0.1%) based on the assumptions used in our simulations and the trajectory data of Lu and Yamada (1998).

To determine if the Las Vegas contribution could change if there was more frequent transport from Las Vegas to Meadview, we simulated a hypothetical scenario by placing the Las Vegas emissions at the Mohave power plant. However, the contribution to sulfate concentrations at Meadview was still small (less than 1%).

#### **4.5 Effect of Cloud Updraft Velocity**

As discussed in Section 2.5.1, we specified cloud updraft velocities to be zero in our base case simulations. This decision was made after performing a number of sensitivity studies with updraft velocities ranging from 5 to 20 cm/s. For all these sensitivity studies, ground-level sulfate concentrations were negligible ( $< 0.01 \mu\text{g}/\text{m}^3$ ), because of transport of pollutants aloft by clouds. Therefore, we used the assumption of zero updraft velocities in all our simulations since it tends to lead to higher ground-level sulfate concentrations.

## 4.6 Effect of Background Concentrations

Because the chemistry in the plume is sensitive to the background concentrations specified, it is useful to determine how the estimated contribution of MPP to sulfate concentrations in the Grand Canyon can change for a plausible variation in background concentrations. We were primarily interested in scenarios that would be conducive to the formation of sulfate in the MPP plume since that would provide an estimate of the upper bound of MPP contributions. Typically, higher background concentrations of VOC, PAN, NO<sub>x</sub> and O<sub>3</sub> should result in faster gas-phase SO<sub>2</sub> conversion rates, particularly near the stack. Similarly, higher aqueous-phase SO<sub>2</sub> conversion rates are expected for higher background concentrations of H<sub>2</sub>O<sub>2</sub> (or equivalently, lower background SO<sub>2</sub> concentrations), trace metals such as iron and manganese (that catalyze aqueous-phase SO<sub>2</sub> oxidation by oxygen), and ammonia (that increases the pH of cloud droplets, thereby enhancing aqueous-phase oxidation by O<sub>3</sub> and O<sub>2</sub>).

We repeated all the base case simulations for Meadview and Hopi Point using the high end of the concentrations measured during Project MOHAVE, except for background SO<sub>2</sub>, which we assumed to be zero in the simulations described here, effectively increasing the amount of background H<sub>2</sub>O<sub>2</sub> available to oxidize plume SO<sub>2</sub>. For species that were not measured, such as aldehydes and PAN, we doubled the base case values. Table 4-1 summarizes the background concentrations used in the study.

Table 4-2 summarizes the results for Meadview. The table shows the base case and high background case model estimates of MPP sulfate concentrations for each 12-hour averaging period that were calculated from the 13 trajectories simulated for Meadview. The relative changes between the high background and base case results and the relative contributions of MPP to the measured sulfate for the high background case are also shown.

We see from Table 4-2 that higher background concentrations do not necessarily result in higher MPP sulfate concentrations at Meadview. The largest increases in MPP sulfate concentrations are predicted for the night of August 5 when aqueous-phase chemistry was the primary mechanism for SO<sub>2</sub> conversion in the plume. Increases in MPP sulfate are also predicted for both the 12-hour periods of August 13. For all the

Table 4-1. High background concentrations (in ppb unless otherwise indicated)

Species	August 6, 1992	August 9, 1992	August 14, 1992
O <sub>3</sub>	55	50	55
NO <sub>2</sub>	5	5	4
H <sub>2</sub> O <sub>2</sub>	1.34	1.34	2.3
SO <sub>2</sub> *	0	0	0
VOC (ppbC)	37.9	115.1	59.5
PAN	0.5	0.5	0.5
CO	408	730	150
NH <sub>3</sub>	5.3	5.3	5.3
Fe (ng/m <sup>3</sup> )	113	113	113
Mn (ng/m <sup>3</sup> )	1.74	1.74	1.74

\* Background SO<sub>2</sub> concentrations are set to zero, effectively increasing H<sub>2</sub>O<sub>2</sub> concentrations available for aqueous-phase oxidation of plume SO<sub>2</sub>.

Table 4-2. High background results for Meadview

<b>Date of initial time</b>	<b>12-hour period</b>	<b>Base Case MPP Sulfate (ng/m<sup>3</sup>)</b>	<b>MPP Sulfate (ng/m<sup>3</sup>) with Higher Background</b>	<b>Change (%)</b>	<b>MPP Contribution (%)</b>
8/5/92	7 p.m. - 7 a.m.	22	97	341	5.9
8/6/92	7 a.m. - 7 p.m.	123	179	46	6.7
8/6/92	7 p.m. - 7 a.m.	31	28	-10	< 1.0
8/8/92	7 p.m. - 7 a.m.	8	7	-13	< 1.0
8/9/92	7 a.m. - 7 p.m.	90	52	-42	2.6
8/13/92	7 a.m. - 7 p.m.	10	13	30	1.0
8/13/92	7 p.m. - 7 a.m.	92	118	28	6.6
8/14/92	7 a.m. - 7 p.m.	244	176	-28	6.1
8/14/92	7 p.m. - 7 a.m.	382	249	-35	12.2
8/15/92	7 p.m. - 7 a.m.	190	154	-19	6.1
8/16/92	7 a.m. - 7 p.m.	53	42	-21	1.7

other 12-hour averaging periods, the higher background concentrations actually result in a decrease in MPP sulfate concentrations at Meadview. In particular, the highest base case MPP sulfate concentration, on the night of August 14, decreases from 382 ng/m<sup>3</sup> to 249 ng/m<sup>3</sup> (a 35% reduction) when higher background concentrations are used. The highest MPP contribution, for the same period, decreases from 19% to 12%.

To understand the reasons for this behavior, we examined the instantaneous sulfate concentrations (for both the base case study and the high background concentration study) in one of the puff trajectories that impacts Meadview during the morning of August 15. Figure 4-4 shows the ratio of the instantaneous plume sulfate concentration in the high background case to the corresponding value in the base case, as a function of travel time. As expected, instantaneous sulfate concentrations near the stack are higher in the high background case than in the base case. However, after about 20 hours of travel, the ratio begins to decrease, ultimately reaching a value of about 0.65 at Meadview, i.e., instantaneous sulfate concentrations in the puff at Meadview are 35% lower in the high background case as compared to the base case.

Figure 4-5 shows the ratio of the instantaneous plume H<sub>2</sub>O<sub>2</sub> concentration in the high background case to the corresponding value in the base case, as a function of travel time. We see that, up to about 20 hours of travel time, the amount of H<sub>2</sub>O<sub>2</sub> produced in the plume for the high background case is essentially identical to that produced in the base case (very little H<sub>2</sub>O<sub>2</sub> is produced in the plume for both cases during this initial period). However, after this initial period, significantly more H<sub>2</sub>O<sub>2</sub> is produced in the high background plume as compared to the base case plume. This suggests that the VOC/NO<sub>x</sub> ratio in the plume for the high background case has reached a level where the formation of H<sub>2</sub>O<sub>2</sub> is favored, resulting in removal of HO<sub>2</sub> radicals from the system, eventually reducing concentrations of the OH radical, the primary gas-phase oxidant for SO<sub>2</sub>. A comparison of the background concentrations in Tables 3-1 and 4-1 shows that the relative increases in NO<sub>2</sub> background concentrations are smaller than the increases in VOC background concentrations when going from the base case to the high background case. In particular, on August 14, the NO<sub>2</sub> background concentration only increases by a little more than 30%, while the VOC background increases by about a factor of 3.

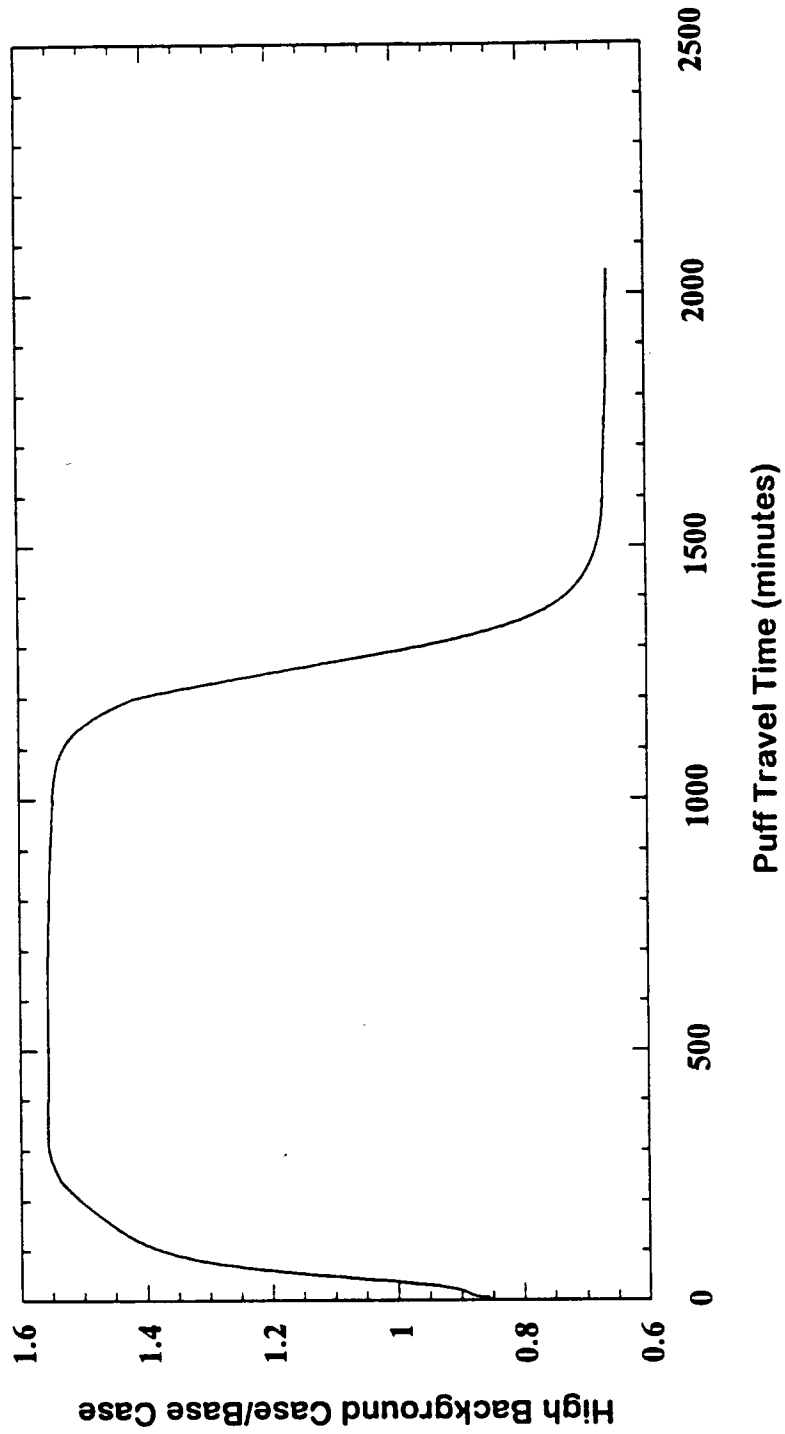


Figure 4-4. The ratio of the instantaneous plume sulfate concentration in the high background case to the corresponding values in the base case, as a function of travel time.

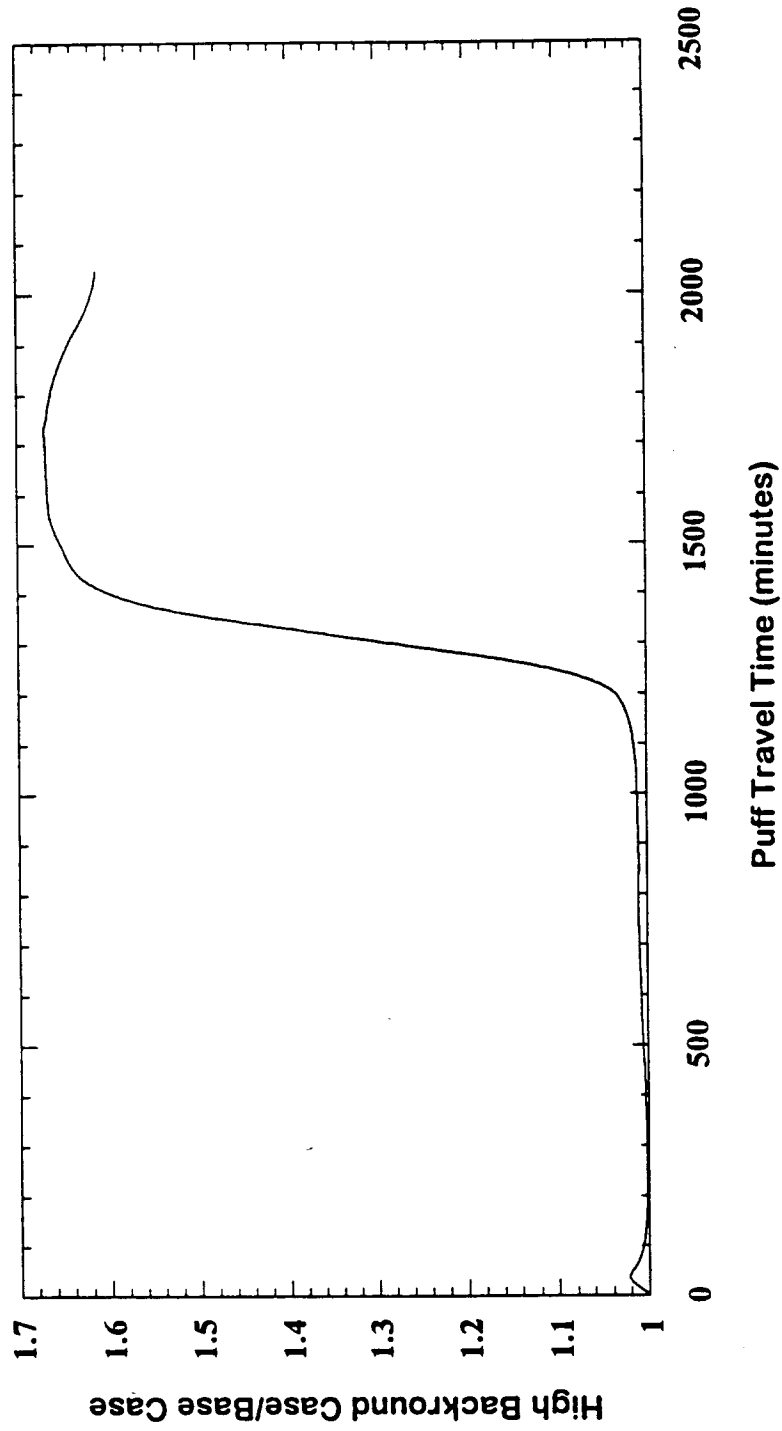


Figure 4-5. The ratio of the instantaneous plume  $H_2O_2$  concentration in the high background case to the corresponding value in the base case, as a function of travel time.

The results for Hopi Point are presented in Table 4-3. As in the case of Meadview, MPP sulfate contributions with the higher background concentrations are generally smaller than the base case contributions.

The above results suggest that, for the background concentrations measured during Project MOHAVE and for sufficiently large plume travel times, MPP sulfate contributions to the Grand Canyon region may be smaller when VOC background concentrations are increased without a commensurate increase in NO<sub>x</sub> concentrations. To determine if the opposite is true, we performed simulations for the August 14 period using clean background conditions, determined as the low end of the concentrations observed during Project MOHAVE. The 12-hour average MPP sulfate concentration and contribution increased by about 16% (from 382 ng/m<sup>3</sup> to 443 ng/m<sup>3</sup> and from 19% to 22%, respectively), when clean background conditions were used.

#### **4.7 Estimation of Maximum Sulfate Concentrations in the Grand Canyon Region**

All our simulations were performed for the Meadview and Hopi Point receptors, primarily because these are the two receptors in the Grand Canyon region where sulfate and MPP tracer concentrations were measured. However, it is of interest to determine the maximum possible MPP sulfate concentration and contribution anywhere in the Grand Canyon region. We used our base case results to get a screening estimate. A more definitive determination would require the use of a gridded Eulerian model, and was beyond the scope of the current study. The approach that we adopted is summarized below.

We examined all trajectories going to Hopi Point. Assuming that the Grand Canyon region begins at a distance corresponding to Meadview and ends at a distance corresponding to Hopi Point, we then extracted the maximum instantaneous sulfate concentration for each trajectory between these two distances. If this maximum concentration occurred at either of the two end points, we assumed that the maximum 12-hour average MPP sulfate concentration in the region corresponded to the base case value at the relevant end point. If the maximum concentration occurred somewhere in between

Table 4-3. High background results for Hopi Point

<b>Date of initial time</b>	<b>12-hour period</b>	<b>Base Case MPP Sulfate (ng/m<sup>3</sup>)</b>	<b>MPP Sulfate (ng/m<sup>3</sup>) with Higher Background</b>	<b>Change (%)</b>	<b>MPP Contribution</b>
8/6/92	7p.m. - 7a.m.	2.1	2.5	19	< 1.0
8/7/92	7a.m. - 7p.m.	16.2	16.7	3	1.0
8/9/92	7 a.m. - 7p.m.	94	67	-29	4.1
8/9/92	7p.m. - 7a.m.	27	20	-26	1.8
8/15/92	7p.m. - 7a.m.	60	48	-20	2.4
8/16/92	7a.m. - 7p.m.	131	93	-29	4.9

the two points, we used the ratio of the maximum instantaneous sulfate concentration to the higher of the instantaneous sulfate concentrations at the two end points to determine a scaling factor that could be used for each trajectory. Finally, we used the maximum scaling factor from all the trajectories influencing a given 12-hour period and applied it to the 12-hour average concentration estimated from the base case study. Table 4-4 shows the ratio of the maximum instantaneous sulfate concentration to the instantaneous sulfate concentration at the higher of the two end-points for all the 10 trajectories going to Hopi Point. We see that the highest ratio is 1.37, corresponding to puff trajectory 500 on August 9. For the period corresponding to the highest base case MPP sulfate concentration at Meadview (i.e., 7 p.m. August 14 to 7 a.m. August 15), we see a peak to receptor ratio of 1.15 corresponding to puff trajectory 1479 on August 16. Figure 4-6 shows the instantaneous sulfate concentrations in the plume between the two end-points for this trajectory, relative to the instantaneous concentration at Hopi Point.

We used this ratio with the highest estimated MPP sulfate concentration ( $382 \text{ ng/m}^3$ ) at Meadview, for the morning of August 15, to get an upper bound estimate of  $439 \text{ ng/m}^3$  for MPP sulfate anywhere in the region, an increase of  $57 \text{ ng/m}^3$ . We assumed that the sulfate concentration measured at Meadview increased by the same amount, resulting in a maximum MPP 12-hour average sulfate contribution of 21% anywhere in the Grand Canyon region.

A complementary analysis was conducted where trajectories that reached Meadview were extended further up to a distance equivalent to that of Hopi Point (but at a different location because of different wind trajectories). If the sulfate concentration along the puff trajectory increased after leaving Meadview, we used the higher puff concentration to calculate the 12-hour average concentrations at Meadview. This approach provides an upper bound estimate since it is assumed that all puffs interact after Meadview in the same manner as they do at Meadview, i.e., we do not account for divergence of individual puff trajectories. No change in the maximum contribution of the MPP plume was obtained in that analysis. The mean 12-hour average MPP sulfate concentration increased to  $152 \text{ } \mu\text{g/m}^3$  and the corresponding contribution to total sulfate increased from 5% to 7%.

Table 4-4. Approximate maximum MPP sulfate concentrations in Grand Canyon region relative to calculated receptor concentrations

<b>Date</b>	<b>Trajectories</b>	<b>Max. MPP Sulfate/MPP Sulfate at Meadview or Hopi Point</b>
August 7, 1992	165	1.00
	176	1.05
	210	1.02
	223	1.00
August 9, 1992	500	1.37
	508	1.23
August 16, 1992	1479	1.15
	1617	1.00
	1693	1.00
	1750	1.00

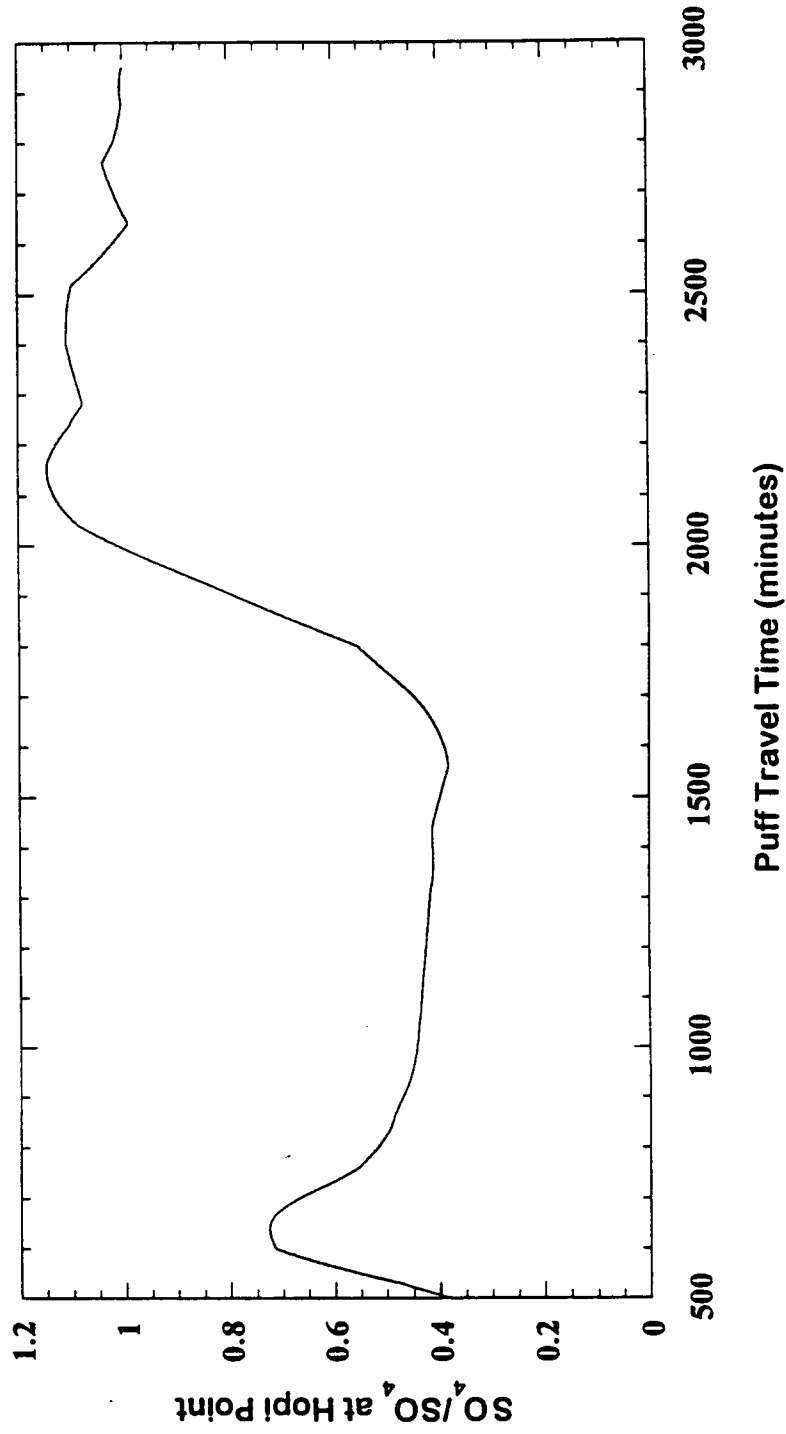


Figure 4-6. Instantaneous sulfate concentrations in the plume in the Grand Canyon region, relative to the instantaneous concentration at Hopi Point for puff 1479.

## 4.8 Effect of Clouds

The base case results and tracer measurements showed that high MPP sulfate concentrations were not predicted for periods in which puffs interacted with clouds, primarily because there was infrequent transport of the MPP plume toward the Grand Canyon during those periods (primarily on August 5 and 6) and the puffs were fast moving with short residence times. Instead, the highest concentrations were predicted for August 14 and August 15, when there was frequent transport of the MPP plume and the puffs had long travel times and residence times in the Grand Canyon region.

To estimate the MPP sulfate contribution for a hypothetical scenario in which puffs interacting with clouds were associated with frequent transport to Meadview and long travel and residence times, we conducted sensitivity simulations by varying the cloud fields along individual puff trajectories. These studies were designed to determine plausible upper bound estimates of MPP sulfate concentrations and contributions.

We performed four separate studies for puff trajectories arriving at Meadview during the 12-hour sampling period from 7 a.m. to 7 p.m. August 6, 1992. Note that three trajectories were tracked for this period in our base case simulations. Of these, one trajectory interacted with cloud, while the other two did not. The trajectory that interacted with clouds encountered clouds for approximately 25% of its travel time from the stack to the receptor. The 4 sensitivity studies that we performed and the impact (relative to the base case results) are listed below:

1. Clouds for cloudy trajectory were applied to the 2 non-cloudy trajectories, i.e., all 3 trajectories interacted with cloud for 25% of their travel time. For this, scenario, the MPP sulfate concentration and contribution increased from 123 to 126 ng/m<sup>3</sup> and 4.6% to 4.7%, respectively.
2. Clouds were specified as in study 1 above, but background SO<sub>2</sub> concentrations were set to zero. This effectively increases H<sub>2</sub>O<sub>2</sub> concentrations available for oxidizing plume SO<sub>2</sub>. The MPP sulfate concentration and contribution increased from 123 to 276 ng/m<sup>3</sup> and 4.6% to 10.3%, respectively.

3. All 3 trajectories were assumed to interact with clouds for 50% of their travel time. The MPP sulfate concentration and contribution increased from 123 to 219 ng/m<sup>3</sup> and 4.6% to 8.2%, respectively.
4. Clouds were specified as in study 3 above, but background SO<sub>2</sub> concentrations were set to zero. The MPP sulfate concentration and contribution increased from 123 to 474 ng/m<sup>3</sup> and 4.6% to 17.7%, respectively.

#### **4.9 Estimation of Maximum Hourly MPP Sulfate Contribution**

To determine the maximum hourly MPP sulfate contribution at Meadview, we took advantage of the fact that high resolution tracer measurements were available at the site. We assumed that the ratio of the maximum hourly and 12-hour average concentrations was the same for the tracer and MPP sulfate. First, the ratio of the maximum hourly tracer concentration to the 12-hour average tracer concentration for the period containing the maximum hourly concentration was determined. This ratio was then used to determine a maximum hourly MPP sulfate concentration using the maximum base case 12-hour MPP sulfate concentration at Meadview (382 ng/m<sup>3</sup>). This yielded a maximum hourly sulfate concentration of 888 ng/m<sup>3</sup>, an increase of 506 ng/m<sup>3</sup> over the 12-hour average value. Assuming that the total maximum hourly sulfate concentration was higher than the 12-hour average value by the same amount, (i.e., the background non-MPP sulfate concentration remains the same over the 12-hour period) we get an estimate of the maximum hourly MPP sulfate contribution of 35%.

## 5. SUMMARY AND CONCLUSIONS

This report describes the application of a reactive plume model to simulate the formation of sulfate in the Mohave Power Plant plume for a 11-day summer period in 1992 during which transport of emissions from the power plant to the Grand Canyon region was indicated by tracer measurements at a number of locations, particularly Meadview, at the western boundary of Grand Canyon National Park.

The meteorology and plume dispersion data for the simulations were developed using the results of Lu and Yamada (1998) who used a prognostic three-dimensional meteorological model and a three-dimensional Lagrangian puff dispersion model to simulate meteorology, turbulence and tracer gas concentrations for the 11-day period. Background chemistry data were obtained from surface and upper air measurements during the period obtained from the Project MOHAVE database. In addition, a survey of the literature of previous measurements in similar regions was performed to specify background concentrations for species such as aldehydes and PAN, that were not measured during Project MOHAVE. MPP emissions of SO<sub>2</sub>, NO<sub>x</sub>, and tracer were also obtained from the Project MOHAVE database. Emissions of trace metals such as iron and manganese were derived from the SO<sub>2</sub> emissions and ratios of MPP Fe and Mn to SO<sub>2</sub> in the stack.

Base case simulations were performed to estimate the contribution of MPP emissions to sulfate concentrations at two receptors in the Grand Canyon region, Meadview and Hopi Point. For practical reasons, a limited number of puff trajectories were selected for plume chemistry analysis from the more than 2000 puff trajectories developed by Lu and Yamada (1998) for the period. The trajectories were selected for days when the largest MPP tracer concentrations were measured. Other criteria for the selection of trajectories included their potential for interaction with clouds, their proximity to the receptors, and the horizontal extent of the puffs. For Meadview, 13 trajectories were simulated and for Hopi Point, 10 trajectories were simulated. The background chemical concentrations for the base case simulations were in the middle of the range of their plausible values. For the base case simulations, several assumptions were made that maximize the conversion of MPP SO<sub>2</sub> emissions to sulfate in order to

develop upper bound estimates of MPP contributions to sulfate concentrations at the receptors. For example, clouds were assumed to exist whenever the cloud water amount diagnosed by Lu and Yamada (1998) exceeded a very low cut-off level of  $0.01 \text{ g/m}^3$ . Also cloud updraft velocities were specified to be zero, since sensitivity studies showed that ground level concentrations were negligible for non-zero updraft velocities.

In addition to the base case simulations, a number of simulations and analyses were conducted to examine the impact of MPP for a number of hypothetical and/or plausible scenarios, as well as to determine the impact of emissions from Las Vegas on sulfate concentrations in the Grand Canyon. For the latter case, we had to make assumptions about  $\text{SO}_2$  emissions from Las Vegas as well as the background VOC,  $\text{NO}_x$ , PAN, and  $\text{O}_3$  concentrations.

Some of the important results from the study are summarized below:

- The maximum 12-hour average base case MPP sulfate concentration and sulfate contribution at Meadview were calculated to be  $382 \text{ ng/m}^3$  and 18.8%, respectively for the 12-hour period from 7 p.m. August 14 to 7 a.m. August 15, 1992. For Hopi Point, the maximum 12-hour average base case MPP sulfate concentration and sulfate contribution were  $129 \text{ ng/m}^3$  and 6.4%, respectively for the 12-hour period from 7 a.m. August 16 to 7 p.m. August 16, 1992.
- The MPP plume had significant interaction with clouds only for puff trajectories released during the night of August 5, 1992 and traveling to Meadview. These trajectories were fast moving and had short residence and impact times at Meadview. None of the trajectories from MPP to Hopi Point encountered clouds at plume levels.
- As expected, increasing the interaction of puff trajectories with clouds increases the conversion of  $\text{SO}_2$  to sulfate in the plume. This effect is enhanced when the  $\text{H}_2\text{O}_2$  available for aqueous-phase oxidation is implicitly increased by setting background concentrations of  $\text{SO}_2$  to zero. For an extreme hypothetical scenario, the upper bound value for the MPP sulfate contribution for a cloudy day was 18%.

- The estimated average molar ratio of MPP sulfate to MPP SO<sub>2</sub> at Meadview is about 9%, about a factor of 3 lower than the corresponding ratio at Hopi Point. This ratio is an approximate measure of the extent of conversion of SO<sub>2</sub> to sulfate in the MPP plume.
- The NO<sub>x</sub> in the plume suppresses SO<sub>2</sub> oxidation rates near the stack. Further downwind, as the plume gets diluted, the effect of plume NO<sub>x</sub> on SO<sub>2</sub> chemistry becomes less important.
- The impact of Las Vegas emissions on sulfate concentrations at Meadview was negligible for the assumptions and trajectory data used in our analysis.
- Changing the background concentrations to favor sulfate formation in the plume (e.g., increasing VOC, O<sub>3</sub>, PAN, Fe, Mn, and NH<sub>3</sub> concentrations and decreasing background SO<sub>2</sub> concentrations) did not always result in higher sulfate concentrations at Meadview or Hopi Point. Further analysis showed that sulfate concentrations at the receptors increased for short trajectories or trajectories interacting with clouds. For the longer trajectories, none of which interacted with clouds, sulfate concentrations in the plume when higher background concentrations were used were initially higher as compared to the base case values. However, as the plume approached the receptors, sulfate formation rates dropped since the plume became NO<sub>x</sub>-limited, leading to increased formation of H<sub>2</sub>O<sub>2</sub> and lower acid (including sulfate) formation in the plume.
- Using a limited number of puff trajectories ending at Hopi Point, the maximum 12-hour average MPP sulfate concentration anywhere in the Grand Canyon region was approximately estimated to be 439 ng/m<sup>3</sup>. This corresponds to an approximate maximum contribution of 21%.
- Using tracer measurements with high time resolution, the maximum 1-hour average MPP sulfate concentration at Meadview was approximately estimated to be 888 ng/m<sup>3</sup>, corresponding to an approximate maximum hourly contribution of 35%.

## 6. REFERENCES

- Altshuller, A.P., 1983. Measurements of the products of atmospheric photochemical reactions in laboratory studies and in ambient air: relationships between ozone and other products, *Atmos. Environ.*, **17**, 2383-2427.
- Ames, R.B. and W.C. Malm, 1997. Estimating the contribution of the Mohave coal-fired power plant emissions to atmospheric extinction at Grand Canyon National Park. Presented at the AWMA/AGU International Specialty Conference on Visual Air Quality, Aerosols and Global Radiation Balance, September 9-12, 1997, Bartlett, New Hampshire.
- Atkinson, R. and A.C. Lloyd, 1984. Evaluation of kinetic and mechanistic data for modeling of photochemical smog, *J. Phys. Chem. Ref. Data*, **13**, 315-444.
- Dawson, G.A. and J.C. Farmer, 1988. Soluble atmospheric trace gases in the southwestern United States, *J. Geophys. Res.*, **93**, 5200-5206.
- Eatough, D.J., R.J. Farber and J.G. Watson, 1997a. Second generation Chemical Mass Balance source apportionment of sulfur oxides and sulfate at the Grand Canyon during the Project MOHAVE 1992 summer intensive, Presented at the AWMA/AGU International Specialty Conference on Visual Air Quality, Aerosols and Global Radiation Balance, September 9-12, 1997, Bartlett, New Hampshire.
- Eatough, D.J., B. Sun, M. Eatough, J. Joseph, J.D. Lamb, N.F. Mangleson and L.B. Rees, 1997b. Chemical profiles of SO<sub>x</sub>, HF, spherical fly ash particles, and fine particle constituents in emissions from coal-fired generating stations in the vicinity of the Grand Canyon, Submitted to *Environ. Sci. Technol.*
- Fahey, D.W., G. Hübler, D.D. Parrish, E.J. Williams, R.B. Norton, B.A. Ridley, H.B. Singh, S.C. Liu and F.C. Fehsenfeld, 1986. Reactive nitrogen species in the troposphere: measurements of NO, NO<sub>2</sub>, HNO<sub>3</sub>, particulate nitrate, peroxyacetyl nitrate (PAN), O<sub>3</sub>, and total reactive odd nitrogen (NO<sub>y</sub>) at Niwot Ridge, Colorado. *J. Geophys. Res.*, **91**, 9781-9793.
- Gabruk, R.S., I. Sykes, C. Seigneur, P. Pai, P. Gillespie, R.W. Bergstrom and P. Saxena, 1999. Performance evaluation of the Reactive & Optics Model of Emissions (ROME), *Atmos. Environ.*, **33**, 383-399.
- Gaffney, J.S., N.A. Marley and E.W. Prestbo, 1993. Measurements of peroxyacetyl nitrate at a remote site in the southwestern United States: Tropospheric implications, *Environ. Sci. Technol.*, **27**, 1905-1910.
- Gery, M.W., G.Z. Whitten, J.P. Killus and M.C. Dodge, 1989. A photochemical kinetics mechanism for urban and regional scale computer modeling, *J. Geophys. Res.*, **94**, 12,925-12,956.

- Green, M.C. and I. Tombach, 1997. Use of Project MOHAVE perfluorocarbon tracer data for source attribution analysis, Presented at the AWMA/AGU International Specialty Conference on Visual Air Quality, Aerosols and Global Radiation Balance, September 9-12, 1997, Bartlett, New Hampshire.
- Grosjean, D., 1991. Ambient levels of formaldehyde, acetaldehyde, and formic acid in southern California: Results of a one-year base-line study, *Environ. Sci. Technol.*, **25**, 710-715.
- Grosjean, D., 1997. Personal communication, DGA, Ventura, CA.
- Hartsell, B.E., V.P. Aneja and W.A. Lonneman, 1994. Relationships between peroxyacetyl nitrate, O<sub>3</sub>, and NO<sub>y</sub> at the rural Southern Oxidants Study site in central Piedmont, North Carolina, site SONIA, *J. Geophys. Res.*, **99**, 21,033-21,041.
- Hegg, D.A., P.V. Hobbs and J.H. Lyons, 1985. Field studies of a power plant plume in the arid southwestern United States, *Atmos. Environ.*, **19**, 1147-1167.
- Hoffman, M.R. and J.G. Calvert, 1985. Chemical Transformation Modules for Eulerian Acid Deposition Models, II. The Aqueous-Phase Chemistry, NCAR Report, National Center for Atmospheric Research, Boulder, CO.
- Hudischewskyj, A.B. and C. Seigneur, 1989. Mathematical modeling of the chemistry and physics of aerosols in plumes, *Environ. Sci. Technol.*, **23**, 413-421.
- Karamchandani, P., P. Pai, A. Venkatram and I. Tombach, 1996. Development and Evaluation of a Model for Predicting Air Quality on the Colorado Plateau. ENSR Report 8700-465-300 prepared for the Grand Canyon Visibility Transport Commission, ENSR Consulting and Engineering, Camarillo, CA.
- Latimer, D.A., 1993. Development of regional haze screening models, Paper 93-TP-49.04, presented at the 86th Annual Meeting of the Air and Waste Management Association, Denver, CO.
- Lu, X. and T. Yamada, 1998. Numerical simulations of airflows and tracer transport in an arid western mountainous area, presented at the 10th AMS Joint Conference on the Applications of Air Pollution Meteorology with the A&WMA, Phoenix, AZ.
- Martin, L., 1994. Aqueous sulfur (IV) oxidation revisited, In: Environmental Oxidants, *Adv. Environ. Sci. Tech.*, **28**, 221-268, J.O. Nriagu and M.S. Simmons, Eds., John Wiley & Sons, Inc., New York, NY.
- Pitchford, M., 1997. Personal communication, U.S. Environmental Protection Agency, Las Vegas, NV.

- Pitchford, M., H. Kuhns, M. Green and R. Farber, 1997. Characterization of regional transport and dispersion using Project MOHAVE tracer data, presented at the AWMA/AGU International Specialty Conference on Visual Air Quality, Aerosols and Global Radiation Balance, September 9-12, 1997, Bartlett, New Hampshire.
- Richards, L.W., J.A. Anderson, D.L. Blumenthal, A.A. Brandt, J.A. McDonald, N. Waters, E.S. Macias and P.S. Bhardwaja, 1981. The chemistry, aerosol physics, and optical properties of a western coal-fired power plant plume, *Atmos. Environ.*, **15**, 2111-2134.
- Richards, L.W., J.A. Anderson, D.L. Blumenthal, A.A. Brandt and J.A. McDonald, 1982. Nitrogen and sulfur chemistry and aerosol formation in plumes, presented at the 75th Annual Meeting of the Air Pollution Control Association, New Orleans, LA.
- Roberts, J.M., R.L. Tanner, L. Newman, V.C. Bowersox, J.W. Bottenheim, K.G. Anlauf, K.A. Brice, D.D. Parrish, F.C. Fehsenfeld, M.P. Buhr, J.F. Meagher and E.M. Bailey, 1995. Relationships between PAN and ozone at sites in eastern North America. *J. Geophys. Res.*, **100**, 22,821-22,830.
- Schulam, P., R. Newbold and L.A. Hull, 1985. Urban and rural ambient air aldehyde levels in Schenectady, New York, and on Whiteface Mountain, New York. *Atmos. Environ.*, **19**, 623-626.
- Seigneur, C. and P. Saxena, 1988. A theoretical investigation of sulfate formation in clouds, *Atmos. Environ.*, **22**, 101-115.
- Seigneur, C. and A.M. Wegrecki, 1990. Mathematical modeling of cloud chemistry in the Los Angeles Basin, *Atmos. Environ.*, **24A**, 989-1006.
- Seigneur, C., X.A. Wu, E. Constantinou, P. Gillespie, R.W. Bergstrom, I. Sykes, A. Venkatram and P. Karamchandani, 1997. Formulation of a second-generation reactive plume & visibility model, *J. Air Waste Manag. Assoc.*, **47**, 176-184.
- Seigneur, C., P. Pai, I. Tombach, C. McDade, P. Saxena and P. Mueller, 1999. Modeling of potential power plant plume impacts on Dallas-Fort Worth visibility, *J. Air Waste Manage. Assoc.*, in press.
- Spicer, C.W., M.W. Holdren and G.W. Keigley, 1983. The ubiquity of peroxyacetyl nitrate in the continental boundary layer, *Atmos. Environ.*, **17**, 1055-1058.
- Tanner, R.L. and Z. Meng, 1984. Seasonal variations in ambient atmospheric levels of formaldehyde and acetaldehyde, *Environ. Sci. Technol.*, **18**, 723-726.

- Ventrakam, A., P. Karamchandani, P. Pai, C. Sloane, P. Saxena and R. Goldstein, 1997. The development of a model to examine source-receptor relationships for visibility on the Colorado Plateau, *J. Air Waste Manage. Assoc.*, **47**, 286-301.
- Vimont, J.C., 1997. Evaluation of the CALMET/CALPUFF modeling system using Project MOHAVE tracer and implications for sulfate, presented at the AWMA/AGU International Specialty Conference on Visual Air Quality, Aerosols and Global Radiation Balance, September 9-12, 1997, Bartlett, New Hampshire.
- Yamada, T. and S. Bunker, 1988. Development of a nested grid, second moment turbulent closure model and application to the 1982 ASCOT Brush Creek data simulation, *J. Appl. Meteor.*, **27**, 562-578.
- Yamada, T., 1997. Numerical Simulations of Airflows and Tracer Transport in the Arid Western Mountainous Area, YSA Report, Yamada Science & Art Corporation, Santa Fe, NM.